Precambrian Research 255 (2014) 716–733

Contents lists available at ScienceDirect

Precambrian Research

journal homepage: www.elsevier.com/locate/precamres

Possible southwestward extrusion of the Ordos Block in the Late Paleoproterozoic: Constraints from kinematic and geochronologic analysis of peripheral ductile shear zones

Wangbin Gong[a,b], Jianmin Hu[a,b,*], Sujuan Wu[a,b], Hong Chen[a,b], Hongjie Qu[a,b], Zhenhong Li[a,b], Yang Liu[c], Lijun Wang[d]

[a] Institute of Geomechanics, Chinese Academy of Geological Sciences, Beijing 100081, China
[b] Key Laboratory of Paleomagnetism and Tectonic Reconstruction of Ministry of Land and Resources, Beijing 100081, China
[c] Kunming University of Science and Technology, Kunming 650093, China
[d] Shandong University of Science and Technology, Qingdao 266510, China

ARTICLE INFO

Article history:
Received 26 November 2013
Received in revised form 11 April 2014
Accepted 2 May 2014
Available online 9 May 2014

Keywords:
Southwestward extrusion
Ordos Block
North China Craton
Ductile shear zone
Late Paleoproterozoic
$^{40}Ar/^{39}Ar$ dating

ABSTRACT

The Paleoproterozoic is a pivotal period of the tectonic evolution of the North China Craton (NCC). Various models have been postulated by previous researchers through the study of petrology and metamorphism, but the lack of structural analyses has hampered further understanding of the tectonic evolution of the NCC. A series of well-exposed ductile shear zones developed on the northern, northwestern and eastern edges of the Ordos Block in the western part of the NCC. We carried out detailed field studies along with isotopic dating focused on the kinematics and geochronology of the ductile shear zones. On the north margin of the Ordos block, the Wulashan-Daqingshan ductile shear zone is characterized by an E-W trending shearing foliation that steeply dips 75–80° to the north or south, with subhorizontal stretching lineation plunging 10–15° toward the east or west and dextral strike-slip shearing kinematics. On the west margin of the Ordos block is the Zongbieli ductile shear zone with top-to-the-NW thrusting kinematics. On the east margin of the Ordos block is the Xueling ductile shear zone with top-to-the-SE thrusting accompanied by sinistral strike-slip shearing kinematics.

The ^{40}Ar–^{39}Ar ages of deformed minerals from mylonitic high-grade metamorphic rocks and LA-ICP-MS U-Pb dating results of zircons from syn-tectonic anatectic granites reflect that the ductile shear zones surrounding the Ordos block deformed between 1.85 and 1.81 Ga. The similar deformation ages indicate that the ductile shear zones might be genetically correlated. The geometry, kinematics and geochronology characteristics of the Wulashan-Daqingshan ductile shear zone on the north margin, the Zongbieli ductile shear zone on the west margin, and the Xueling ductile shear zone combined with the Zhujiafang sinistral ductile shear zone on the east margin defined the possible southwestward extrusion of the Ordos block in the late Paleoproterozoic, which might have resulted from the westward subduction-collision of the Eastern Block under the Western Block at approximately 1.85 Ga and which is correlated with the amalgamation of the Columbia supercontinent.

1. Introduction

The North China Craton (NCC) is one of the oldest cratonic blocks in the world (Zhao and Zhai, 2013; Diwu et al., 2013), and the Precambrian tectonic evolution and continental growth in the NCC have been discussed in a number of recent works (Wilde et al., 2002, 2004; Wilde and Zhao, 2005; Kröner et al., 2005; Kusky and Li, 2003; Kusky et al., 2007; Santosh et al., 2006, 2007a,b, 2008, 2009a,b,c, 2010; Wan et al., 2013a; Zhao et al., 1998, 2001, 2002a, 2003a, 2005, 2006, 2009; Zhai and Santosh, 2011; Hu et al., 2013; Li et al., 2005, 2006, 2010, 2011a,b, 2012; Li and Zhao, 2007; Wu et al., 2012, 2013). There is no consensus about its subdivision or the tectonic models for the formation and evolution of the craton (Zhao and Zhai, 2013).

Four main models have been described in terms of field-based metamorphic, geochemical, geophysical and geochronological

* Corresponding author at: Institute of Geomechanics, Chinese Academy of Geological Sciences, Beijing 100081, China. Tel.: +86 010 88815003; fax: +86 10 68422326.
E-mail address: jianminhu@vip.sina.com (J. Hu).

http://dx.doi.org/10.1016/j.precamres.2014.05.001
0301-9268/

studies: (1) Zhai (2011) proposed a two-stage cratonization model of the NCC. The first stage took place at the end of the Neoarchean at ~2.5 Ga, when several micro-blocks were amalgamated. The second cratonization event consisted of cratonic reworking corresponding to a rifting-subduction-collision at 2.3–1.97 Ga and subsequent extension-uplifting related to upwelling mantle at 1.97–1.82 Ga, which might be linked to the assembly and breaking up, respectively, of the Columbia Supercontinent. (2) Zhao et al. (2002a, 2005) proposed that three Paleoproterozoic orogenic belts existed in the NCC. The Khondalite Belt resulted from the amalgamation of the Yinshan and Ordos Blocks to form the Western Block at ~1.95 Ga, whereas the Trans-North China Orogen resulted from a collision of the Western and Eastern blocks above an eastward subduction zone at ~1.85 Ga. The Jiao-Liao-Ji Belt records opening and closing of an intra-continental rift within the Eastern Block in the period 2.2–1.9 Ga (Li et al., 2005, 2006, 2011a,b, 2012; Li and Zhao, 2007; Tam et al., 2012a,b; Wu et al., 2012, 2013). (3) Faure et al. (2007) and Trap et al. (2007, 2008, 2009a,b, 2011, 2012) postulated that an old continental block named the Fuping Block intervenes between the Eastern and Western (Ordos) Blocks, which were separated from the Fuping Block by the Zanhuang Ocean and the Lüliang Ocean, which closed at ~2.1 and 1.9–1.8 Ga, respectively, and both of which were subducted westward. (4) Kusky et al. (2007) proposed that the northern margin of the craton experienced a continental collision with part of the Columbia supercontinent (South America) at 1.93–1.92 Ga, followed by the development of an extensive craton-wide rift system at 1.85–1.80 Ga.

That the Paleoproterozic is a pivotal period for the tectonic evolution of the NCC can be inferred from the above models despite their differences. And almost all of the points were obtained from the analyses of three Paleoproterozoic linear structural belts developed in the North China Craton (Zhang et al., 1994, 2007, 2009; Faure et al., 2007; Trap et al., 2007, 2008, 2009a,b, 2011, 2012; Li et al., 2010, 2012). Among these, the "Khondalite Belt" (Zhao et al., 2002a, 2005), which is also known as the "Fengzhen Orogenic Belt" (Zhai and Peng, 2007; Zhai and Santosh, 2011) or the "Inner Mongolia Suture Zone" (part of the Khondalite Belt/Fengzhen Belt) (Santosh et al., 2010), and the "Trans-North China Orogen" (Zhao et al., 2002a, 2005), which is also known as the "Jinyu Orogenic Belt" (Zhai and Peng, 2007; Zhai and Santosh, 2011), are located on the north and east margins of the Ordos block, respectively (Fig. 1). Studies of its petrology and metamorphism have provided abundant information about the evolution of the NCC, whereas few investigations on the structural deformation of the NCC have been conducted (Trap et al., 2007, 2008, 2009a,b, 2011, 2012; Zhang et al., 2007). The lack of structural data has further hampered understanding of the Precambrian evolution of the NCC.

Ductile shear zones consisting of strike-slip ductile shear zones, large-scale thrusting and folding, and transcurrent tectonics are extensively exposed in the Paleoproterozoic linear structural belts of the NCC (Yu and Sun, 1996; Liu et al., 2007; Chen et al., 2008; Trap et al., 2007, 2008, 2009a,b, 2011, 2012; Zhang et al., 2007), which may provide important information about the crustal structure and the regional structure (Isik, 2009).

In this paper, we report detailed field studies focused on the geometry and kinematics along with LA-ICP-MS U–Pb analyses of zircon and $^{40}Ar/^{39}Ar$ dating of deformed minerals in three ductile shear zones: the Wulashan-Daqingshan ductile shear zone, the Zongbieli ductile shear zone and the Xueling ductile shear zone located on the northern, the northwestern and the eastern margins of the Ordos Block, respectively (Fig. 1). The geometry, kinematics and geochronology characteristics of the ductile shear zones defined the possible southwestward extrusion of the Ordos block, indicating that the North China Craton underwent a complicated structural process during the late Paleoproterozoic.

2. Wulashan-Daqingshan strike-slip ductile shear zone

2.1. General geological features

2.1.1. Main stratigraphic unit

The Wulashan-Daqingshan area is located on the north margin of the Ordos block in the central part of the EW-trending Khondalite Belt (Fig. 1). The Precambrian basement was originally divided into the Sanggan Group, the Wulashan Group and metamorphosed magmatic units (Fig. 2) (Yang et al., 2003). The metamorphosed magmatic units include garnet granite, augen granitic gneiss, charnockite and tonalite-granodiorite gneiss. The Sanggan Group is composed mainly of granulite facies supracrustal rocks of Late Neoarchean age (Ma et al., 2012) (Fig. 3). Granulite series are composed of various granulites, pyroxene plagioclase gneiss and magnetite quartzite, and the primary rocks are a sequence of mafic-felsic volcanic and sedimentary rocks (Liu et al., 2007). The Wulashan Group was divided into the Upper and Lower Wulashan Subgroups (Fig. 3), of which the lower subgroup, a meta-volcano-sedimentary association, was considered to have formed during the Archean (Yang et al., 2003). The Upper Wulashan Subgroup is composed of the "Khondalite Series" including metamorphosed clastic sediments, calc-silicate rocks, marbles, garnet-biotite gneiss and some basic igneous rocks (Dong et al., 2013a,b), which represent passive continental margin metasediments (Condie et al., 1992). The garnet-biotite gneiss unit was named as the Daqingshan Supracrustal rocks by Dong et al. (2013a). Recent SHRIMP and LA-ICP-MS U–Pb zircon ages revealed that the sedimentary protoliths of the Khondalite Series were deposited in the period of 2.3–1.95 Ga and experienced high-grade granulite facies (HT-HP and HT-UHT) metamorphism at 1.97–1.82 Ga (Dong et al., 2012, 2013a,b; Wan et al., 2006; Xia et al., 2006a,b, 2008, 2009; Yin et al., 2009, 2011; Li et al., 2011a,b; Guo et al., 2012; Santosh et al., 2007a,b, 2009a,b; Zhai and Santosh, 2011; Zhai, 2011).

2.1.2. Structural framework

The Wulashan-Daqingshan area mainly consists of the late Archean Wulashan group and Sanggan group high-grade metamorphic rocks and late Paleozoic granites. A series of parallel ductile shear zones developed along the trend of the orogen and anatectic granite veins were emplaced along the regional gneissic and shearing foliation, which compose the main architecture of the Wulashan-Daqingshan area. Field investigations indicate that the ductile shear zones are mainly distributed along the contacts of different tectonic units or within the late Archean Wulashan group and Sanggan group metamorphic complex. The widths of the E-W trending ductile shear zones vary from decameters to kilometers. In the central part of Wulashan, both the anatectic granite veins and the ductile shear zone are cut by late Carboniferous granites. The largest Dahuabei pluton intruded at 353 ± 7 Ma (Miao et al., 2001). To the east, the ductile shear zone is covered by the Jurassic basin and was disturbed by late Mesozoic thrusting (Fig. 2).

2.2. Syn-tectonic anatectic granite veins

The western part of Wulashan has numerous anatectic plutons consisting of gneissic anatectic biotite monzonitic granites, K-feldspar granites and gneissic quartz diorites which intruded along the gneissic foliation of the Wulashan group gneiss. The geometry of the anatectic plutons is different from the late Paleozoic Dahuabei pluton. The anatectic plutons have a strip geometry and are 10–25 km long and 1–2 km wide with a length:breadth ratio of approximately 10:1 (Fig. 2). The narrow strips of anatectic granite veins developed along the gneissic foliation at outcrop scales (Fig. 4).

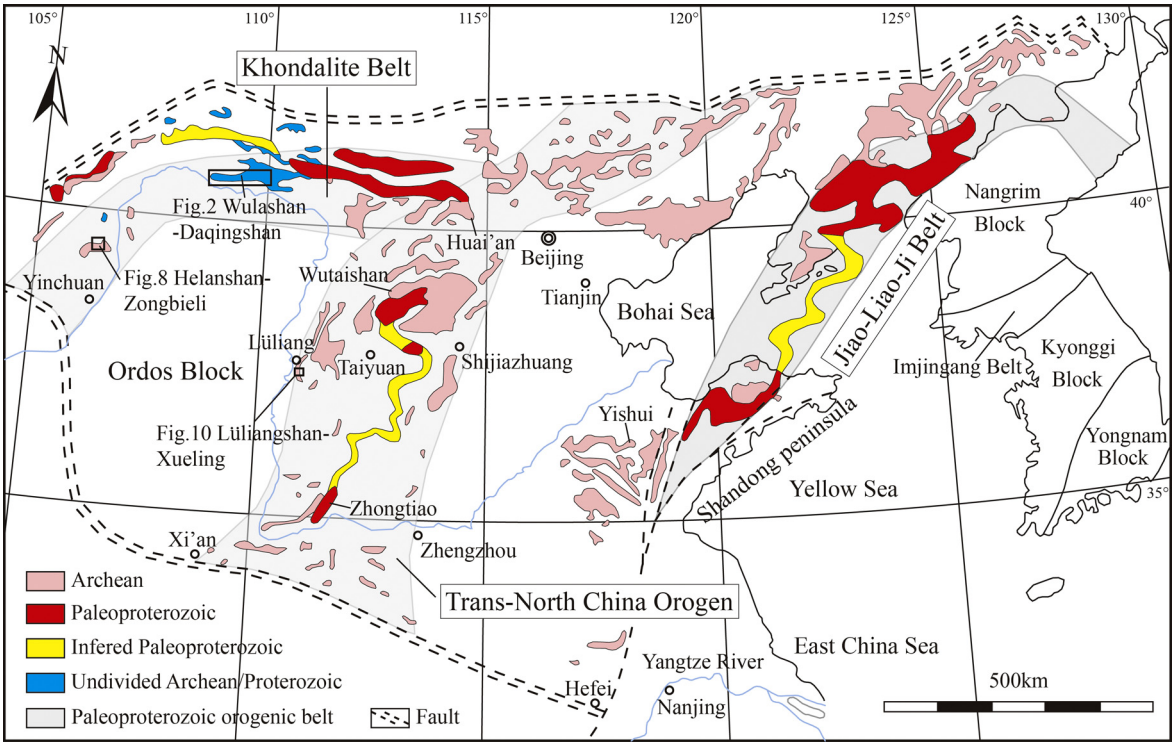

Fig. 1. Sketch map showing the distribution of Paleoproterozoic orogenic belts and ductile shear zones in the North China Craton discussed in this paper (modified from Zhai and Santosh, 2011; Zhai, 2011; Zhao et al., 2002, 2005; Li et al., 2006; Li and Zhao, 2007).

At Mositingamu east of Wulateqianqi, the E-W trending banded anatectic granite veins are harmonious with the regional structures (Fig. 2). The intrusion of anatectic granite veins along the gneissic foliation of the Lower Wulashan Subgroup gneisses resulted in the migmatization of the surrounding rocks (Fig. 4). Granite structural lenticulars developed between the granite and gneiss. The granitic vein is characterized by gneissic and augen structures, which consist of stretched and crushed feldspar and quartz showing the characteristics of syn-tectonic intrusion. The book-shelf structures, asymmetric folded leucosome veins, rotated K-feldspar porphyroblasts and S-C fabrics that developed in the gneiss and anatectic granite indicate dextral shearing (Fig. 4).

2.3. Characteristics of ductile shear zones

Subvertical foliations with subhorizontal lineations are the main characteristics of this ductile shear zone together with asymmetric rotated porphyroclasts, mineral fishes, S-C fabrics, and asymmetric garnet pressure shadows, which indicate dextral strike-slip shearing.

2.3.1. Geometry characteristics

The E-W trending and NEE trending shearing foliation parallel the regional gneissic foliation and steeply dip 75–80° to the north or the south. The subhorizontal stretching lineation includes oriented amphibolites, biotites and stretched quartz ribbons. The plunge of the lineation is 10–15° toward the E or W and shows strike-slip shearing kinematics (Figs. 2 and 5). In the central part of the Wulashan-Daqingshan area, the strike of the shearing foliation changes from NE to N-S as a result of the effects of brittle faults; the lineation is similar to the others and shows strike-slip shearing (Fig. 2, NOR43 and NOR122).

2.3.2. Kinematic indicators

Asymmetric rotated porphyroclasts, quartz ribbons, feldspar fishes and asymmetric garnet pressure shadows are typical kinematic indicators of the Wulashan-Daqingshan ductile shear zone. The oriented biotites and quartz ribbons in the deformation belt comprise the gneissic and banded structures. Unlike the typical mylonite in the shallow-moderate crust, most of the minerals of the deformed rocks in the ductile shear zone have been recrystallized.

(1) *Asymmetric garnet pressure shadows*. Garnets are extensively developed in the khondalite rocks of the Wulashan-Daqingshan area and are preserved as the asymmetric garnet pressure shadow, which resulted from the ductile shearing and indicates dextral shearing. The core of the pressure shadow consists of fractured garnet, and the shadow is composed of recrystallized feldspars, biotites and quartz amalgamations that crystallized perpendicularly to the garnet boundary. The flexure of the biotite crystals can be clearly observed in the sections (Fig. 6).

(2) *Quartz ribbons and feldspar fish inclusions*. Quartz ribbons are the typical micro-fabrics in the high-grade metamorphic rocks from the Wulashan-Daqingshan ductile shear zone. Quartz ribbons are thought to be characteristic of high temperature mylonite and resulted from high temperature plastic deformation of quartz grains under granulite facies (Hippertt et al., 2001; Bochez, 1977). Differences in the deformation characteristics of quartzes are controlled by the intensity of stress. In the strongly deformed domain, oriented rectangle and subrectangle quartz grains with feldspar inclusions comprise the quartz ribbons (Fig. 7). In the weakly deformed domain, discrete quartz ribbons with irregular boundaries resulted from kinematic recrystallization (Fig. 7c and d).

The residual porphyroblasts and matrix structure are absent because most of the feldspars have been recrystallized in the shear zone. Two types of deformed feldspar remnants are included in the quartz ribbons: single grain and amalgamation. Both formed feldspar fish and indicate dextral shearing accompanied by quartz ribbons (Fig. 7a and b).

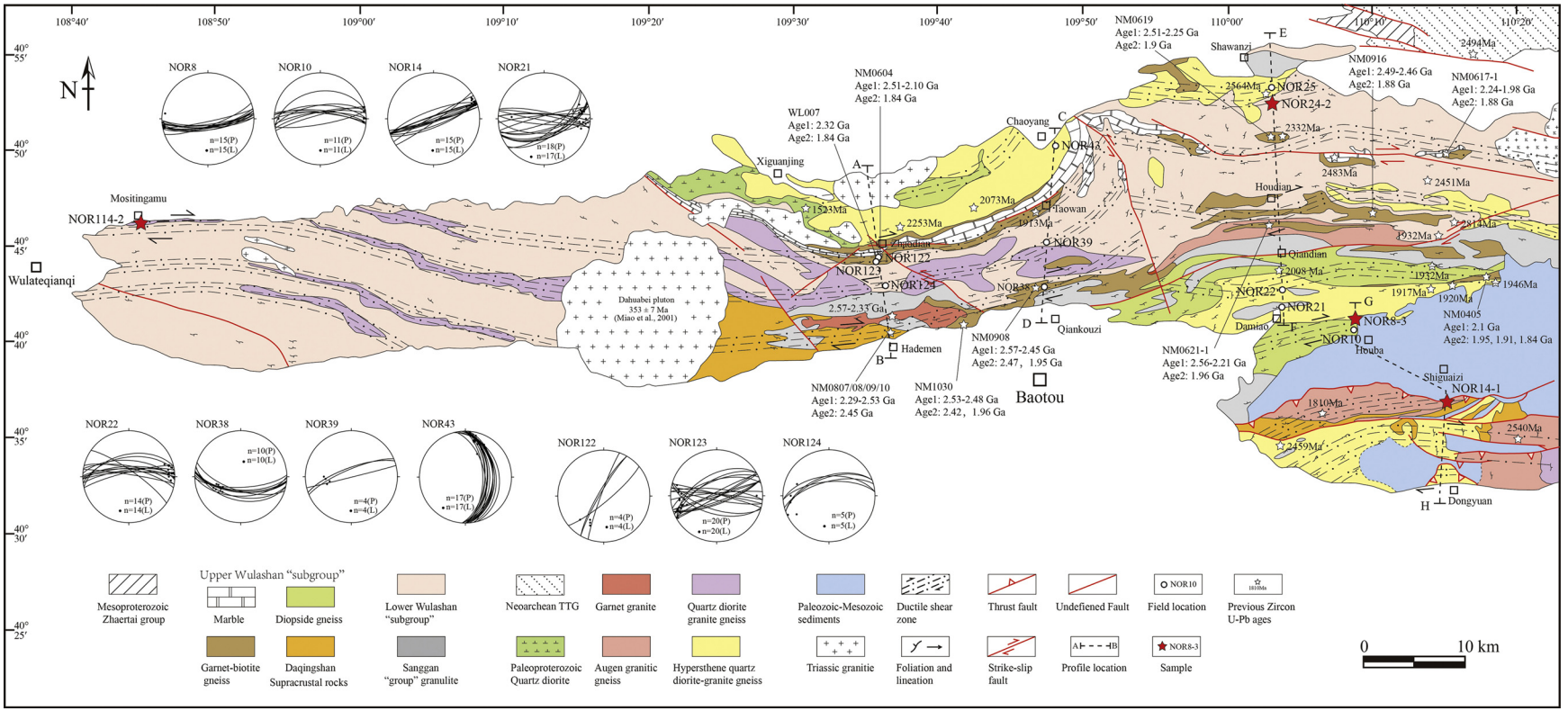

Fig. 2. Geological map of the Wulashan-Daqingshan area showing the ductile shear zones and sample locations (modified from BGMRIMP, 1971; CESJU, 2003; Dong et al., 2013a,b). Zircon U–Pb ages are from Xia et al. (2006a), Wan et al. (2009), and Dong et al. (2013a,b). Age1 is the age of detrital zircon and represents the age of the formation. Age2 is the age of metamorphic or anatectic zircon and represents the time of the tectonothermal event. The SHRIMP zircon U–Pb age of Dahuabei pluton is from Miao et al. (2001). Polar stereographic projections of foliation and stretching lineation are equal-area lower hemisphere projections; the large circle girdles and spots represent tectonic foliation and lineation, respectively.

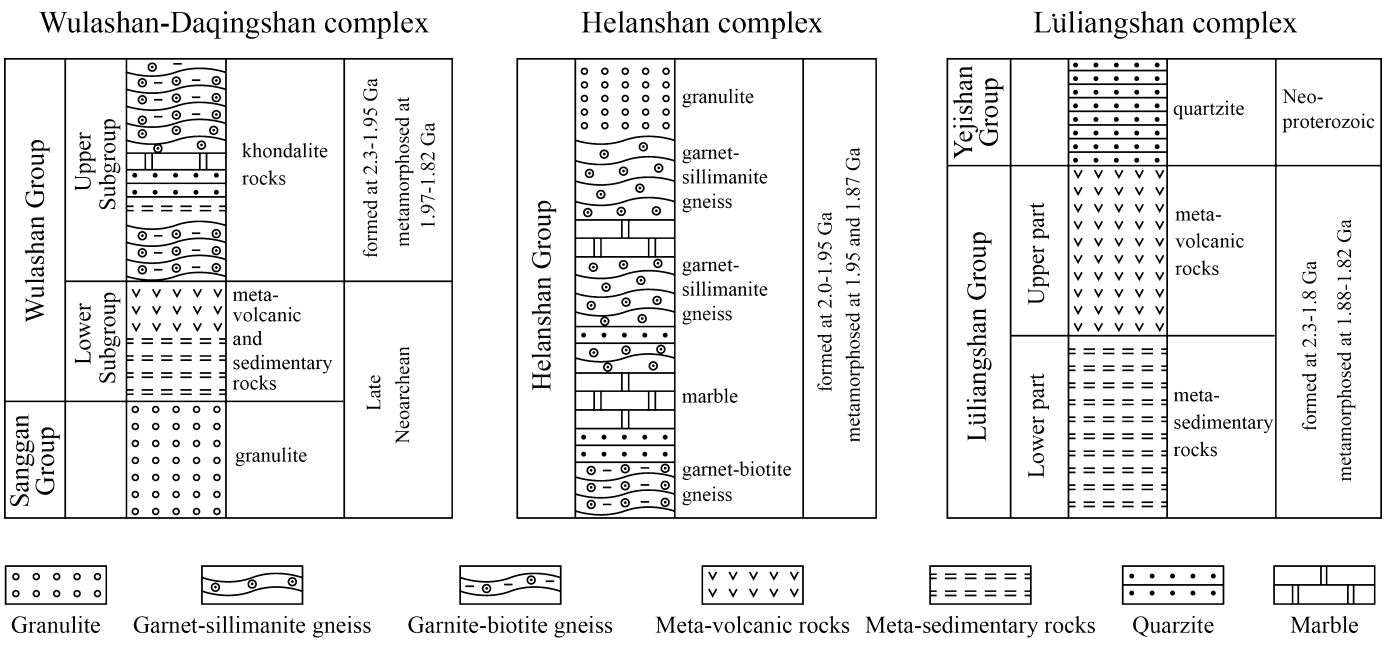

Fig. 3. The sequences of Precambrian metamorphic rocks at the Ordos edges where the ductile shear zones occurred.

3. The Zongbieli ductile shear zone

3.1. Main stratigraphic unit

The Zongbieli area is located in the northern part of the Helanshan complex, which lies in the western part of the khondalite belt at the west margin of the Ordos Block (see Fig. 1 for location). The Helanshan Complex is composed of high-grade Al-rich gneisses, migmatites, S-type granites, quartzite, minor marble and calc-silicate rocks, which together compose the Helanshan group (Yin et al., 2011) (Fig. 3). The protoliths of the Helanshan group are high-grade metamorphic rocks deposited 2.0–1.95 Ga, which underwent two metamorphic events at ~1.95 Ga and ~1.87 Ga (Yin et al., 2011). The S-type granites include garnet-bearing granites and

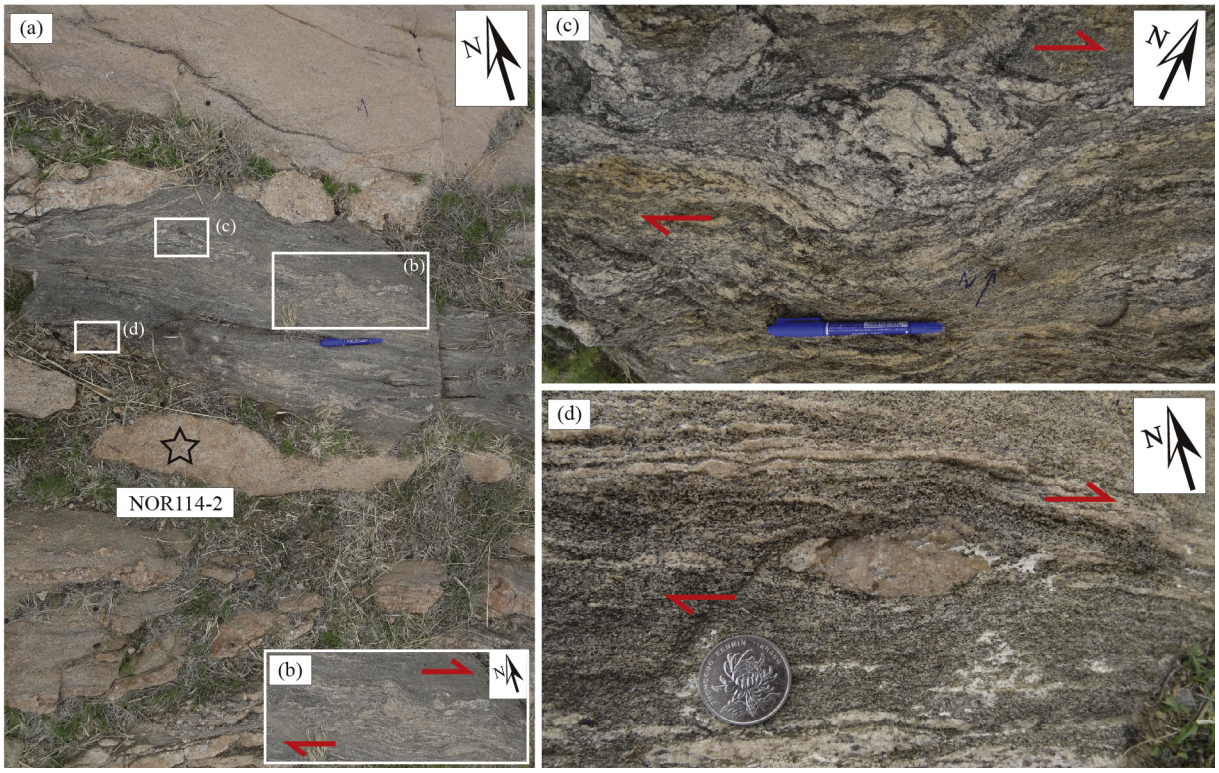

Fig. 4. Field photographs of the syn-tectonic anatectic granite, the surrounded Lower Wulashan subgroup magmatic gneiss and kinematic indicators, which indicate dextral ductile shearing in the Wulashan-Daqingshan area (NOR114, GPS coordinates: N40°45′36.1″/E108°47′19.7″). (a) Lenticular anatectic granite intruded along the gneissic foliation of migmatic gneiss. (b) Asymmetric folded leucosome veins. (c) Anatectic leucosome formed a book-shelf structure. (d) Rotated K-feldspar. porphyroclasts. Top view; coin (2.5 cm in diameter) and pencil (10 cm long) for scale.

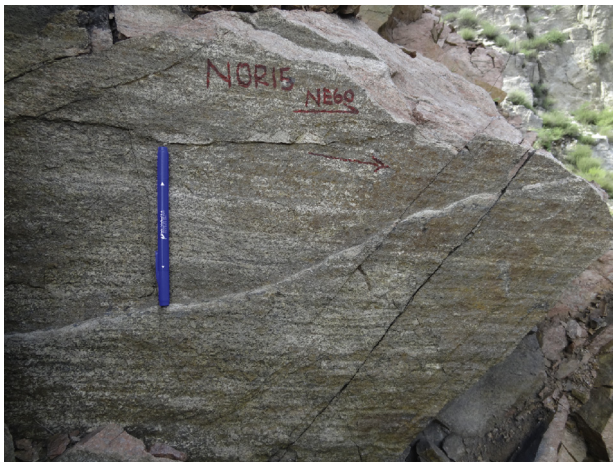

Fig. 5. Field photo of subhorizontal lineation on the steeply dipping foliation. Pencil (10 cm long) for scale.

garnet-bearing granitic migmatites emplaced during the Paleoproterozoic according to an Rb–Sr isotopic dating age of 1793 ± 34 Ma (BGMRNP, 1991) and U–Pb zircon ages of 1858 ± 23 Ma and 1840 ± 15 Ma (Yin et al., 2011) (Fig. 8).

3.2. Characteristics of the ductile shear zone

The NE-striking Zongbieli ductile shear zone consists of several parallel zones with widths of 10–100 m. It developed mainly in high-grade metamorphic rocks of the Helanshan group. In general, the boundaries of the shear zones are transitional, but locally sharp boundaries do exist. The effect of the shear zone resulted in the formation of mylonites, mylonitic gneisses, banded granulites and narrow zones of granites.

The mylonitic rocks in the shear zone are characterized by penetrative foliation and lineation. The mylonitic foliation is defined by flattened and oriented quartzes, biotites and feldspar aggregates. It strikes NE to NEE and dips 60–80° to the SE. The mineral lineation developed on the shearing foliations is defined mainly by quartz ribbons and aggregates of biotite and plunges 60° to the SE (Fig. 8). The S-type granites and garnet-bearing granitic migmatites occur as NE-trending discontinuous narrow zones along the shear zones in the central and southern part of the Zongbieli area, which shows a relationship between the emplacement of granites and the deformation of the ductile shear zone.

The mylonized rocks in the Zongbieli ductile shear zone are generally composed of matrix and porphyroclasts. The porphyroclasts in the granitic mylonites are dominated by plagioclase, K-feldspar, garnet and lenticular quartz grains. The matrix materials include recrystallized quartz, feldspar and biotite. The quartz porphyroclasts show undulose extinction, a lenticular shape and corroded boundaries, which are surrounded by a kinematic recrystallized grain aggregate. The biotites are oriented to form the biotite fishes (Fig. 9b). The shear sense indicators, such as asymmetric feldspar porphyroclasts observed in the outcrop scales (Fig. 9a), S-C fabric and biotite fishes observed in the micro-scales (Fig. 9b) accompanied by foliation and lineation indicate top-to-the-NW thrusting.

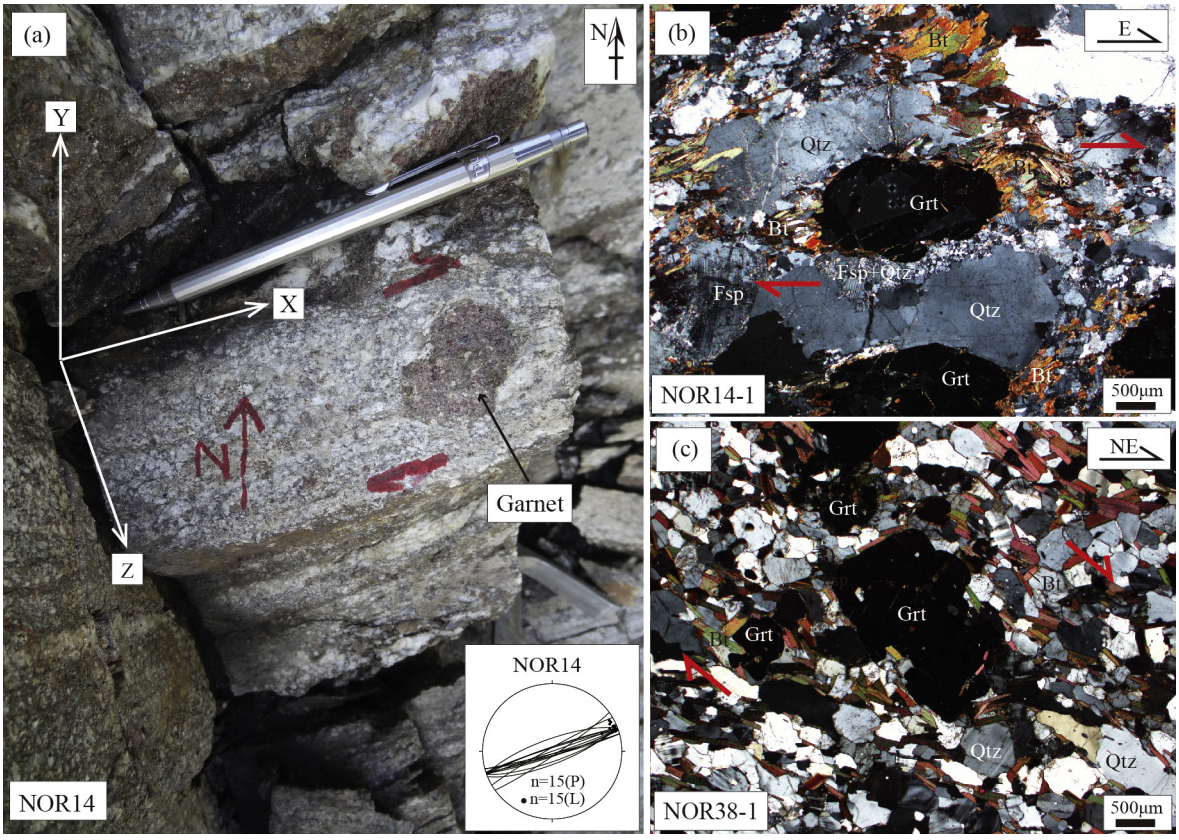

Fig. 6. Asymmetric garnet pressure shadows in Wulashan-Daqingshan ductile shear zone, northern part of west NCC. (a and b) Field and microscope characteristics of asymmetric garnet pressure shadow (NOR14, GPS coordinates: N40°38′59.6″/E110°17′10.7″); oriented feldspars, quartzes and biotites comprise the asymmetric pressure shadow. (c) Microphoto of asymmetric garnet pressure shadow in NOR38 (GPS coordinates: N40°43′5.7″, E110°10′22.5″). Cross-polarized light; section parallel to the lineation and normal to the foliation.

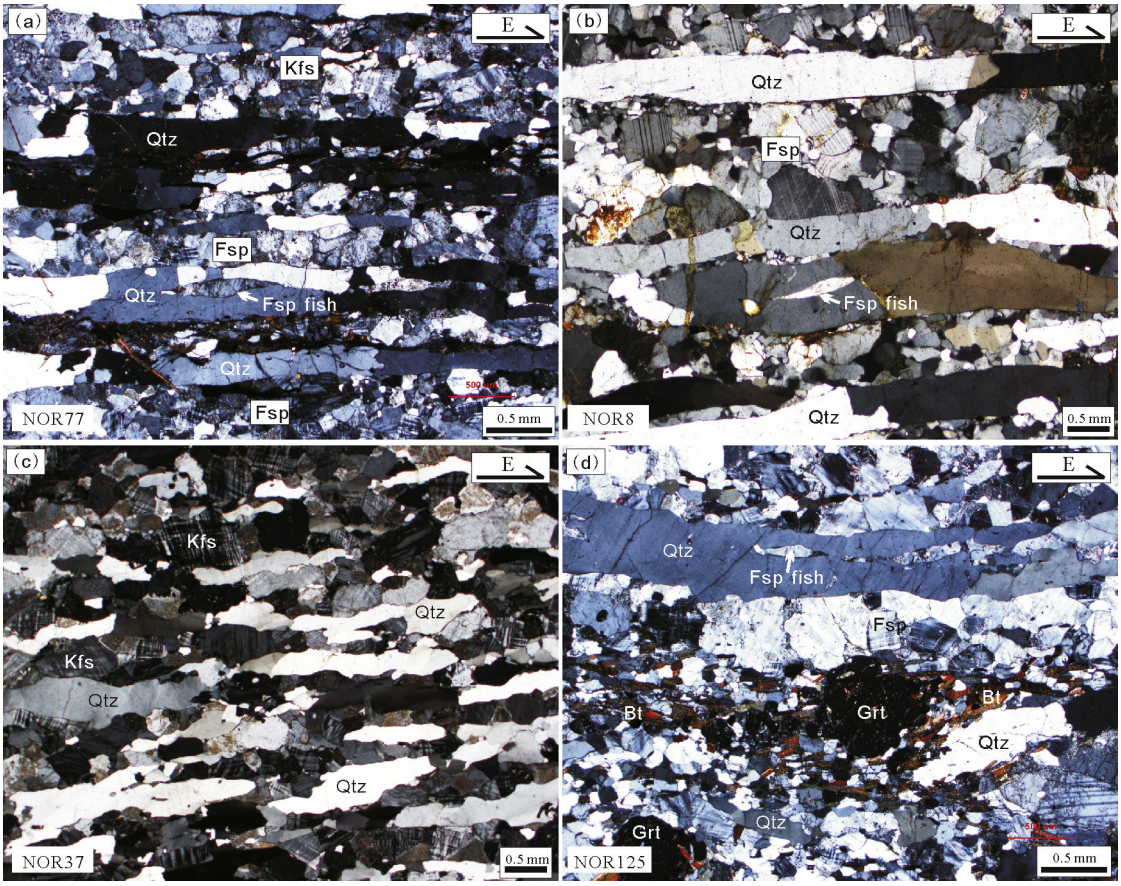

Fig. 7. Quartz ribbons in ductile shear zone. (a and b) Polycrystalline quartz ribbons with straight boundaries cutting across the surrounding feldspar grains and containing inclusions of feldspars (NOR77, GPS coordinates: N40°55′16.1″/E110°3′34.4″; NOR8, GPS coordinates: N40°43′5.7″/E110°10′22.5″). (c) Discrete quartz ribbons with irregular boundaries (NOR37, GPS coordinates: N40°43′9.1″/E109°48′48.7″). (d) Polycrystalline quartz ribbons and asymmetric garnet pressure shadow with garnet core and mantle composed of oriented biotites, recrystallized quartzes and feldspars (NOR125, GPS coordinates: N40°43′9.1″/E109°48′48.7″). Cross-polarized light; sections parallel to the lineation and normal to the foliation.

4. The Xueling ductile shear zone

4.1. Main stratigraphic unit

The Xueling area is located in the northwestern part of the Lüliang complex which lies on the central part of the Tran-North China Orogen at the east margin of the Ordos block (see Fig. 1 for location). The Lüliang complex includes five major lithological units which mainly formed in the period of 2.3–1.8 Ga (Yu and Wang, 1999; Geng et al., 2000, 2003, 2004; Wan et al., 2000) and metamorphosed at 1.88–1.82 Ga (Liu et al., 2006). The Xueling area hosts the Lüliangshan group, which consists of greenshist- to amphibolite-facies meta-sedimentary rocks in the lower part and meta-volcanic rocks in the upper part (Yu et al., 1997) (Fig. 3), which erupted from 2.05 to 2.36 Ga (Yu et al., 1997; Geng et al., 2000). The Lüliangshan group is unconformably covered by weakly metamorphosed Neoproterozoic Yejishan Group quartz sandstones, unmetamorphosed Paleozoic limestones and Cenozoic sediments. NNE-trending faults dip to NNW-thrust Precambrian rocks to Paleozoic limestones (Fig. 10).

4.2. Characteristics of ductile shear zone

The Xueling ductile shear zone developed in the Paleoproterozoic granitic gneisses to the west of the Zhike country and the weakly metamorphosed Neoproterozoic quartz sandstones were not disturbed. The penetrative shearing foliation defined by the flattened and stretched biotites and quartz ribbons parallels the gneiss foliation with a N30E strike and dips moderately to the NW. The strike and plunge of the stretching lineation defined mainly by the oriented biotites are consistent toward the NW and dip 40–50° toward the NW (Fig. 10b), respectively. Metamorphic rocks of the Lüliangshan group exhibit both mesoscopic and microscopic features typical of deformation due to ductile shearing. Two types of mylonites have been observed in the Xueling shear zone: mylonite and augen-bearing protomylonite (Fig. 11). Mesoscopic rotated asymmetric K-feldspar porphyroclasts in the augen-bearing proto mylonites indicate top-to-the-SE thrusting accompanied by sinistral shearing (Fig. 11c). Microscopic S-C fabric defined by oriented biotites and quartz porphyroclasts indicate the same kinematics.

5. Geochronological data

LA-ICP-MS U–Pb dating on zircon was used to determine the age of the syn-tectonic anatectic granite in Wulashan-Daqingshan ductile shear zone. Mylonite and mylonitic rock samples were selected for ^{40}Ar–^{39}Ar dating to refine the age of ductile shear deformation.

5.1. Zircon U–Pb LA-ICP-MS dating

5.1.1. Analytical techniques

The rocks were crushed in a ring mill and sieved (400 μm). Non-magnetic and slightly magnetic heavy minerals were separated

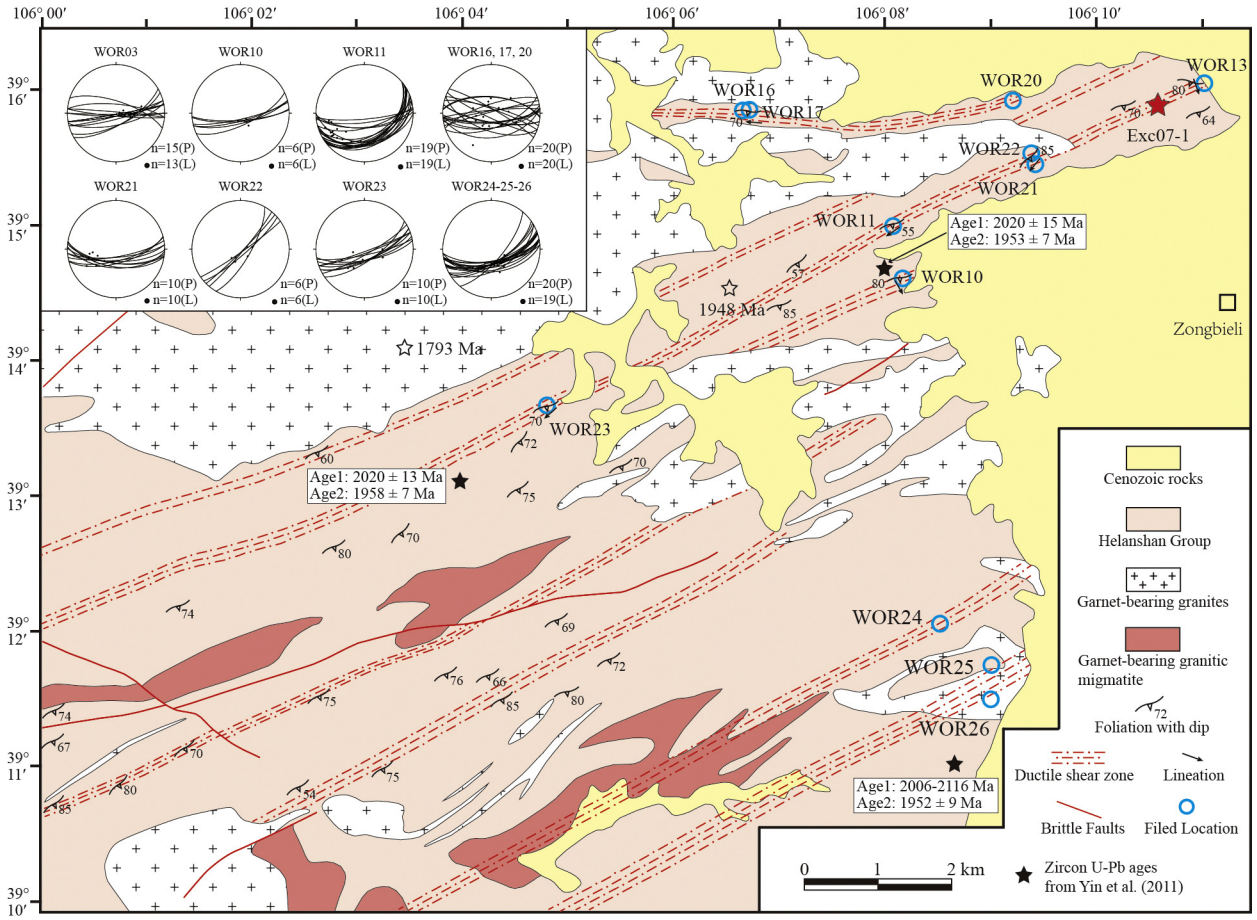

Fig. 8. Geological map showing the Zongbieli ductile shear zones on the west margin of the Ordos block (modified from BGMRNP, 1991). Age1 is the age of detrital zircon coming from the source rocks, which can define the depositional age of the high-grade metamorphic rocks; Age2 is the age of the regional metamorphism. The polar stereographic projections of foliation and lineation are equal-area lower hemisphere projections; the large circle girdles and spots represent tectonic foliations and lineations, respectively.

from the <400 μm fraction. Large zircon grains were then picked from the heavy mineral separate and mounted in epoxy. The mounts were polished to reveal the grain centers, and all grains were imaged in transmitted and reflected light as well as in cathodoluminescence (CL) to identify internal structures and select the best locations for LA-ICP-MS analysis.

Each sample was analyzed using a (ESI) UP193-FX ArF Excimer laser ablation system (Neptune, Thermofisher Scientific) with a 193-nm wavelength at the Tianjin Institute of Geology and Mineral Resources. The MC-ICP-MS instrument is equipped with nine Faraday cups, including an axial Faraday cup and eight off-axis Faraday cups, and four ion counters. Ablation was performed in

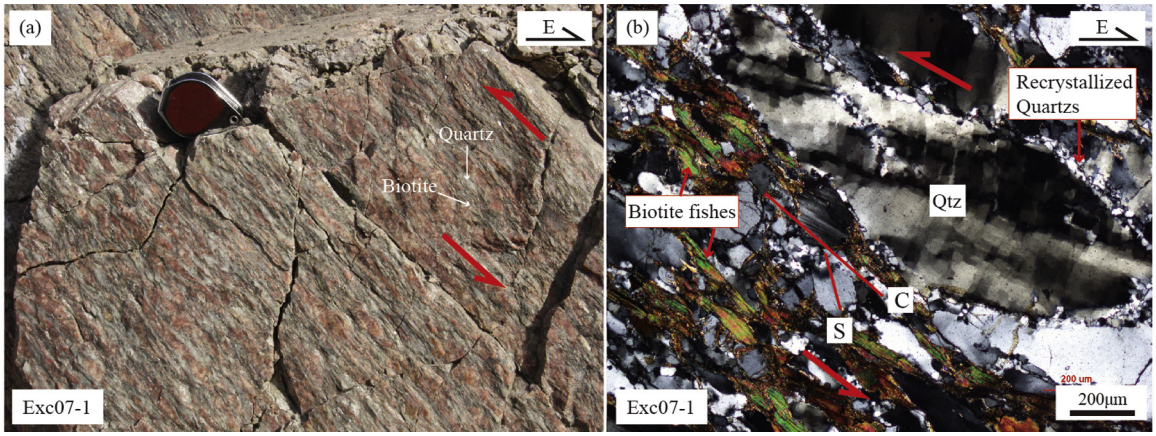

Fig. 9. Kinematic indicators of the Zongbieli ductile shear zone in the Helanshan complex showing top-to-the NW thrusting. (a) Granitic mylonite. (b) Microstructures typical of the Zongbieli ductile shear zone, recrystallized quartzes, undulose extinction, and biotite fishes are observed (cross-polarized light; section parallel to the lineation and normal to the foliation).

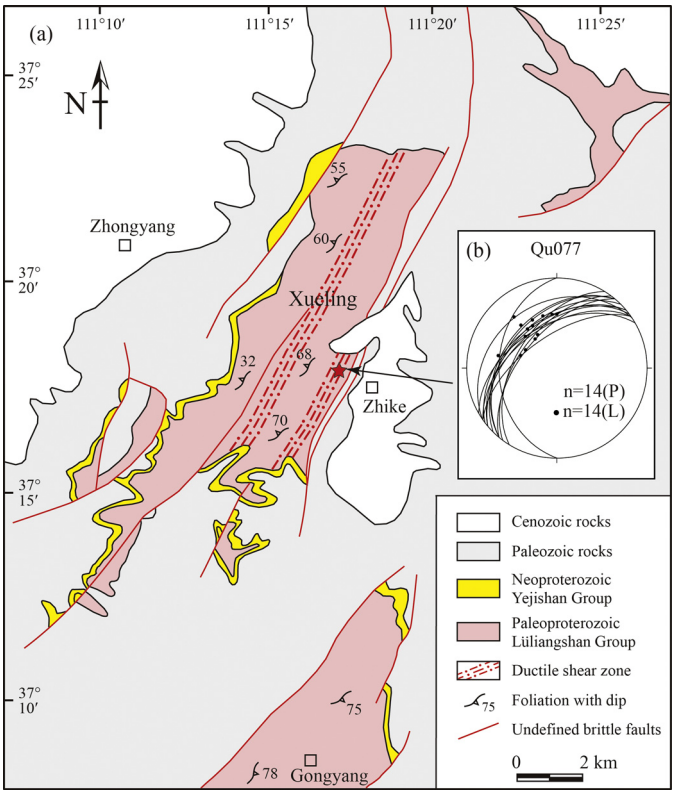

Fig. 10. (a) Simplified geological map of the Xueling area shows the Xueling ductile shear zone and sample locations on the east margin of the Ordos block (modified from BGMRSP, 1976). (b) Foliation and lineation of the Xueling ductile shear zone. The polar stereographic projections are equal-area lower hemisphere projections; the large circle girdles and spots represent tectonic foliations and lineations, respectively.

a custom-designed chamber in a He atmosphere using a laser pulse rate of 8–10 Hz on a beam 35 μm in size delivering approximately 13–14 J cm^{-2}. Mass bias, down hole fractionation and instrumental drift were corrected by analyzing the Temora and GJ-1 international zircon standard (Black et al., 2003; Jackson et al., 2004) for every eight unknown zircons. An NIST612 standard glass sample was applied to calculate the content of Pb, U and Th. ^{208}Pb was applied for the common lead correction (Andersen, 2002). Weighted averages and Concordia plots were calculated using the isoplot software of ICPMS DataCal according to Liu et al. (2009, 2010) and Isoplot (Ludwig, 2003). Individual analyses are presented with 1σ error in the data tables and Condordia diagrams.

5.1.2. Samples and results

Sample NOR114-2 is a medium- to coarse-grained granite collected from syn-tectonic anatectic granite within the Wulashan-Daqingshan ductile shear zone located south of Mositingamu (GPS coordinates: N40°45′41.8″/E108°47′15.4″) (see Figs. 2 and 8 for location). The sample is composed of biotite (15%), quartz (35%), plagioclase (20%) and K-feldspar (25%).

Cathodoluminescence images reveal that nearly all the zircon grains from this sample are euhedral and have no developed cores. Most of the zircon grains are characterized by concentric oscillatory-zoning that was evidently derived from an igneous provenance. The long axis of the zircon is approximately 100–200 μm with a length:breadth ratio of approximately 2:1 to 5:1 (Fig. 12).

The U–Pb analysis results are shown in Table 1. The Th/U ratio of zircon is approximately 0.38–3.62, typical of an igneous origin. Thirteen concordant data points (discordance ≤ 5%) yield a weighted mean $^{207}Pb/^{206}Pb$ age of 1858 ± 21 Ma (n = 13; 95% confidence; MSWD = 0.22; Fig. 13), which is interpreted as the approximate crystallization age of the Mositingamu anatectic granite.

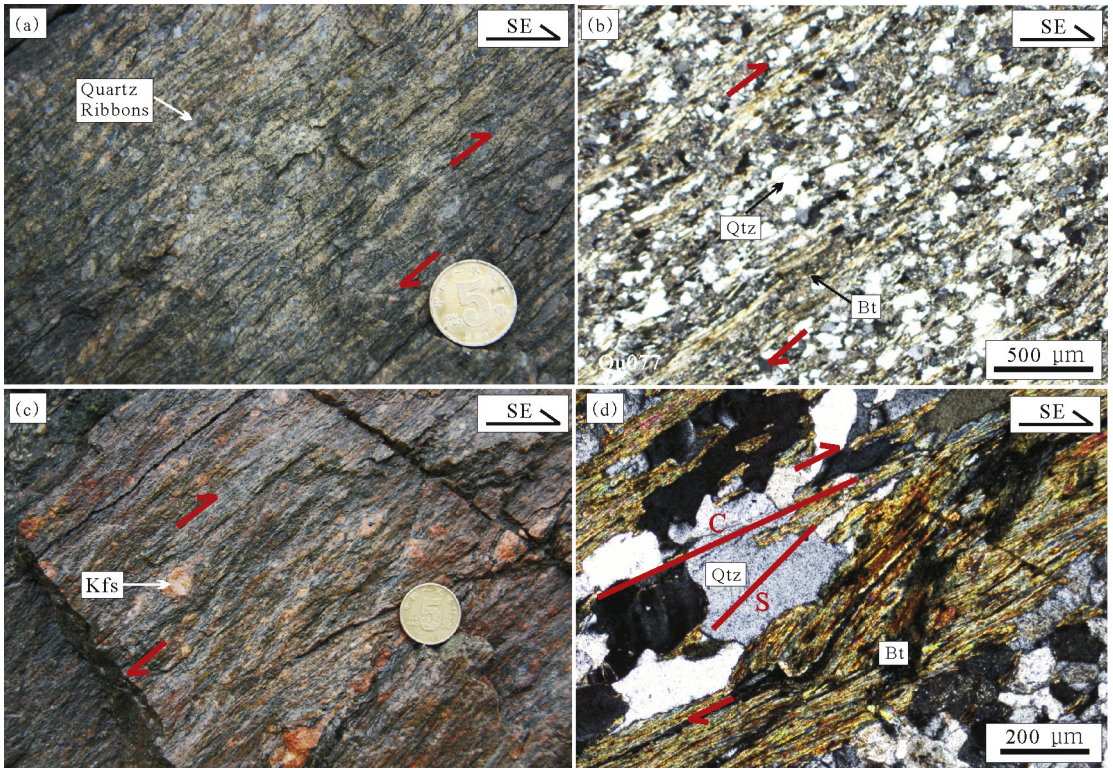

Fig. 11. Mylonites in the Xueling ductile shear zone, shear sense indicators showing top-to-the-SE thrusting. (a) Quartz ribbons and asymmetric porphyroclasts of quartzofeldspathic aggregates in mylonite. (b) Foliation defined by stretched biotites and quartzes. (c) Asymmetric K-feldspar porphyroclasts in augen-bearing protomylonite. (d) S-C fabric defined by oriented biotites and quartz porphyroclasts, respectively (Qu077, GPS coordinates: N37°18′19″/E111°16′45″). Coin (2 cm in diameter) for scale.

Table 1
LA-ICP-MS analyses for zircons from syn-tectonic anatectic granite (sample NOR114-2) along the Wulashan-Daqingshan ductile shear zone.

Test point	Elemental data		Th/U	Isotopic ratios						Ages (Ma)					
	Pb	U		$^{206}Pb/^{238}U$	1σ	$^{207}Pb/^{235}U$	1σ	$^{207}Pb/^{206}Pb$	1σ	$^{206}Pb/^{238}U$	1σ	$^{207}Pb/^{235}U$	1σ	$^{207}Pb/^{206}Pb$	1σ
1	86	218	1.42	0.3206	0.0038	5.0222	0.0641	0.1136	0.0013	1793	21	1823	23	1858	21
2	49	114	1.04	0.3293	0.0031	5.1343	0.0661	0.1131	0.0015	1835	17	1842	24	1850	23
3	168	1137	2.53	0.1086	0.0010	2.8127	0.0350	0.1879	0.0021	664	6	1359	17	2724	18
4	317	942	0.68	0.2772	0.0045	4.3120	0.0566	0.1128	0.0010	1577	25	1696	22	1845	16
5	104	267	0.91	0.3242	0.0038	5.0718	0.0630	0.1135	0.0011	1810	21	1831	23	1856	18
6	168	918	0.74	0.1603	0.0029	3.1197	0.0408	0.1411	0.0017	959	17	1438	19	2241	21
7	142	340	0.91	0.3417	0.0046	5.4036	0.0691	0.1147	0.0014	1895	26	1885	24	1875	22
8	97	228	1.65	0.3042	0.0032	4.7919	0.0636	0.1143	0.0017	1712	18	1783	24	1868	28
9	184	579	0.37	0.2946	0.0056	5.0123	0.0724	0.1234	0.0015	1664	32	1821	26	2006	21
10	194	567	0.65	0.2939	0.0059	4.5455	0.0624	0.1122	0.0012	1661	33	1739	24	1835	19
11	134	525	3.51	0.1803	0.0049	4.3954	0.0719	0.1768	0.0020	1069	29	1711	28	2623	18
12	132	318	1.19	0.3147	0.0049	6.2264	0.0819	0.1435	0.0014	1764	27	2008	26	2270	16
13	90	226	1.33	0.3197	0.0042	5.6646	0.0811	0.1285	0.0019	1788	24	1926	28	2077	26
14	104	232	1.94	0.3218	0.0033	5.2204	0.0670	0.1177	0.0013	1798	18	1856	24	1921	20
15	62	150	0.87	0.3295	0.0032	5.3070	0.0685	0.1168	0.0014	1836	18	1870	24	1908	22
16	25	58	0.67	0.3446	0.0038	5.6252	0.0875	0.1184	0.0030	1909	21	1920	30	1932	46
17	81	229	0.60	0.2848	0.0030	4.8476	0.0620	0.1234	0.0015	1616	17	1793	23	2007	22
18	202	675	0.31	0.2560	0.0026	4.0669	0.0512	0.1152	0.0012	1469	15	1648	21	1883	19
19	190	583	0.27	0.2833	0.0029	4.5071	0.0567	0.1154	0.0011	1608	16	1732	22	1886	18
20	45	119	0.37	0.3246	0.0043	5.0513	0.0681	0.1129	0.0016	1812	24	1828	25	1846	25
21	84	202	0.72	0.3258	0.0037	5.1034	0.0653	0.1136	0.0012	1818	21	1837	23	1858	20
22	76	197	0.51	0.3179	0.0044	5.0039	0.0661	0.1142	0.0013	1779	24	1820	24	1867	21
23	83	190	0.97	0.3338	0.0035	5.4462	0.0731	0.1183	0.0018	1857	19	1892	25	1931	27
24	57	125	0.74	0.3460	0.0038	5.5017	0.0727	0.1153	0.0016	1915	21	1901	25	1885	25

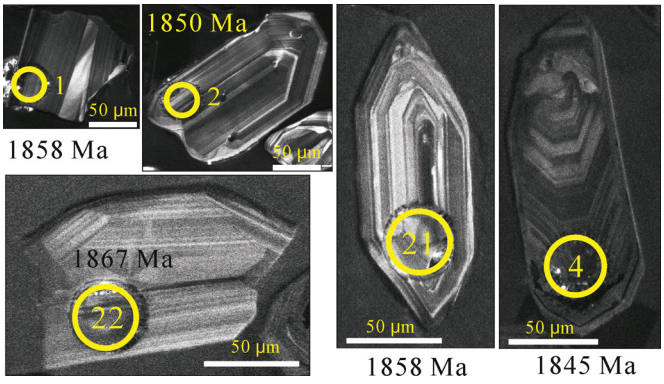

Fig. 12. Cathodoluminescence images of zircons from Paleoproterozoic syn-tectonic anatectic granite in the Wulashan-Daqingshan ductile shear zone.

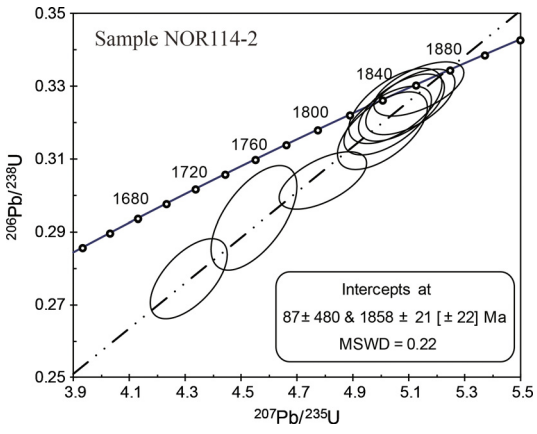

Fig. 13. Concordia diagram of LA-ICP-MS U–Pb zircon data from syn-tectonic anatectic granite in the Wulashan-Daqingshan ductile shear zone.

5.2. $^{40}Ar/^{39}Ar$ dating

5.2.1. Analytical method

Biotite and muscovite grains were separated by conventional heavy liquid and magnetic techniques, and the samples were analyzed by the ^{40}Ar–^{39}Ar incremental heating method in the Nevada Isotope Geochronology Laboratory at the University of Nevada, Las Vegas, USA. Samples were analyzed by the step-heating method utilizing a double vacuum resistance furnace similar to the design of Staudacher et al. (1978). Details of the analytical methods and data treatment are discussed by Justet and Spell (2001) and Spell and McDougall (2003).

5.2.2. $^{40}Ar/^{39}Ar$ sample and results

Three biotite samples from the Wulashan-Daqingshan ductile shear zone, one muscovite sample from the Zongbieli ductile shear zone, and one muscovite sample from the Xueling ductile shear zone were analyzed by ^{40}Ar–^{39}Ar dating (Table 2). Plateau ages were obtained for three samples, and only total gas ages were obtained for the other two samples (Fig. 14).

(1) *Wulashan-Daqingshan ductile shear zone on the north margin of the Ordos block*. Rock sample NOR8-3 is a mylonitic felsic gneiss sampled on the north margin of the Mesozoic Shiguaizi basin (GPS coordinates: N40°43′5.7″/E110°10′22.5″), which consists of quartz (40%), K-feldspar (20%), plagioclase (35%) and biotite (5%). Feldspar amalgamations and quartz ribbons formed the micro-layers and biotites have been deformed into irregular deformation lamellae and altered along the quartz ribbons (Fig. 7b). The hump shape in this sample shows classic alteration; therefore, no plateau age was obtained. The $^{40}Ar/^{39}Ar$ total gas age of the biotite is 1678 ± 12 Ma. A weighted mean age of 1819 ± 14 Ma was obtained from steps 3–15, with 82% of ^{39}Ar released (Fig. 14a).

Rock sample NOR14-1 is a mylonitic garnet biotite gneiss sampled on the south margin of the Mesozoic Shiguaizi basin (GPS coordinates: N40°38′59.6″/E110°17′10.7″), which consists of garnet (15%), biotite (25%), plagioclase (30%), and quartz (30%). There are two different quartz grains, and recrystallization feldspars and deformed biotites oriented around the garnets and formed the asymmetric garnet shadow, indicating dextral shearing (Fig. 7d).

Table 2
^{40}Ar–^{39}Ar dating results.

T (°C)	($^{40}Ar/^{39}Ar$) m	($^{36}Ar/^{39}Ar$) m	($^{37}Ar/^{39}Ar$) m	($^{38}Ar/^{39}Ar$) m	$^{40}Ar^*/^{39}Ar$	^{39}Ar ($\times10^{-12}$ mol)	^{39}Ar/%	Age/Ma (±1sd Ma)
Sample NOR8-3 (Daqingshan-Wulashan ductile shear zone, N40°43′5.7″, E110°10′22.5″)								
Biotite, W = 2.48 mg, J = 0.001798 ± 0.67%								
Total gas age = 1678 ± 12 Ma								
600	267.8729	0.071853	0.011786	0.052234	253.3705	28.085	12.9	677 ± 7
640	696.3593	0.089957	0.008309	0.050307	685.8706	11.072	5.1	1449 ± 13
680	976.0332	0.259249	0.007972	0.085576	923.8543	14.677	6.8	1766 ± 14
710	937.0584	0.046489	0.004328	0.042562	943.7465	12.476	5.7	1790 ± 14
740	942.7903	0.045054	0.004588	0.040936	950.2563	8.501	3.9	1798 ± 14
770	966.9708	0.043378	0.004496	0.04034	975.4406	8.230	3.8	1828 ± 14
820	973.8464	0.042746	0.059279	0.04148	982.5971	13.428	6.2	1836 ± 14
880	986.557	0.03032	0.0047	0.03909	998.7973	17.447	8.0	1855 ± 15
940	1045.664	0.038692	0.009657	0.03928	1057.011	15.326	7.1	1921 ± 15
1000	1024.985	0.016604	0.003856	0.037202	1041.841	28.789	13.3	1904 ± 15
1050	998.9157	0.012273	0.002637	0.033575	1016.428	29.576	13.6	1875 ± 15
1100	979.6415	0.010533	0.003608	0.032123	997.4111	17.184	7.9	1853 ± 14
1150	958.7766	0.007893	0.001535	0.031353	977.4906	9.122	4.2	1830 ± 14
1220	878.9568	0.054054	0.006486	0.037838	886.6851	1.850	0.9	1720 ± 14
1400	870.2564	0.158697	0.008316	0.06237	850.447	1.443	0.7	1674 ± 14
Sample NOR14-1 (Daqingshan-Wulashan ductile shear zone, N40°38′59.6″, E110°17′10.7″)								
Biotite, W = 0.27 mg, J = 0.001802 ± 0.69%								
Plateau age = 1885 ± 20 Ma (9–13 heating steps, 50% of ^{39}Ar released), total gas age = 1678 ± 12 Ma								
600	405.5194	0.277202	0.011658	0.071244	333.0009	0.772	2.2	848 ± 13
650	751.1886	0.116861	0.016694	0.058431	730.725	0.599	1.7	1516 ± 19
700	958.6264	0.064364	0.009419	0.031397	953.548	1.274	3.6	1804 ± 21
750	995.1549	0.030181	0.003622	0.027364	994.9239	2.485	7.0	1853 ± 21
800	993.9547	0.016632	0.002772	0.025179	998.4975	4.329	12.2	1857 ± 21
860	988.0933	0.017237	0.001061	0.026783	991.6079	3.771	10.7	1849 ± 21
920	990.4044	0.024883	0.003888	0.028383	990.5024	2.572	7.3	1848 ± 21
960	976.59	0.032777	0.007476	0.028752	970.2559	1.739	4.9	1824 ± 20
1000	1021.867	0.041353	0.005639	0.031328	1014.626	1.596	4.5	1876 ± 21
1040	1038.648	0.035348	0.004611	0.026127	1034.878	1.952	5.5	1899 ± 21
1090	1114.359	0.021782	0.000849	0.022914	1032.52	3.535	10.0	1896 ± 21
1150	1010.939	0.016607	0.000357	0.025893	1016.156	5.600	15.8	1877 ± 21
1400	1028.502	0.076863	0.001359	0.037461	1018.247	5.152	14.6	1880 ± 21
Sample NOR24-2 (Daqingshan-Wulashan ductile shear zone, N40°54′14.6″, E110°4′16.4″)								
Biotite, W = 0.34 mg, J = 0.001727 ± 0.23%								
Plateau age = 1814 ± 13 Ma (4–13 heating steps, 78% of ^{39}Ar released), total gas age = 1735 ± 11 Ma								
600	497.6014	0.164855	0.011232	0.085145	456.852	2.760	7.4	1049 ± 15
650	802.8614	0.085034	0.009354	0.072279	788.7675	2.352	6.3	1551 ± 18
700	929.2318	0.054498	0.004596	0.064347	925.0746	3.046	8.2	1722 ± 19
750	999.6489	0.030816	0.006062	0.058853	1001.117	3.959	10.7	1811 ± 20
800	1006.832	0.018599	0.003513	0.05683	1012.001	4.839	13.1	1824 ± 20
860	1006.205	0.027945	0.051762	0.056208	1008.562	3.149	8.5	1820 ± 20
920	994.2593	0.049383	0.010101	0.061167	989.37	1.782	4.8	1798 ± 20
960	1004.833	0.081981	0.016225	0.065756	990.6215	1.171	3.2	1799 ± 20
1000	1014.879	0.074474	0.014571	0.072855	1007.413	1.853	5.0	1818 ± 21
1040	1246.053	0.064171	0.014584	0.080214	1022.641	2.057	5.6	1836 ± 20
1090	1014.094	0.038239	0.03117	0.069087	1016.04	3.112	8.4	1828 ± 20
1150	1005.182	0.02034	0.009507	0.056379	1008.959	4.523	12.2	1820 ± 20
1400	1010.024	0.143148	0.02074	0.082147	980.9822	2.459	6.6	1788 ± 20
Sample Exc07-1 (Zongbieli ductile shear zone, N39°15′53″, E106°10′30″)								
Muscovite, W = 0.72 mg, J = 0.002492 ± 0.50%								
Total gas age = 1739 ± 9 Ma								
725	540.326	0.07342	0.00324	0.02742	527.996124	4.631	3.9	1515 ± 9
775	585.279	0.01182	0.00197	0.01548	591.367547	3.552	3.0	1634 ± 10
820	603.323	0.00914	0.00305	0.01577	610.104083	5.580	4.7	1668 ± 10
840	614.69	0.00767	0.0023	0.01515	610.824166	5.213	4.4	1669 ± 10
870	639.711	0.00501	0.00096	0.01289	647.950732	9.390	8.0	1734 ± 10
885	645.388	0.00403	0.00134	0.01459	653.976384	9.666	8.2	1744 ± 10
900	644.302	0.00395	0.00115	0.01325	652.987729	7.848	6.7	1743 ± 10
920	638.746	0.00489	0.00142	0.01404	647.194936	6.338	5.4	1733 ± 10
940	632.562	0.0067	0.00242	0.01414	640.115282	5.374	4.6	1720 ± 10
960	628.317	0.00904	0.00397	0.01522	635.196662	4.533	3.8	1712 ± 10
980	635.827	0.00933	0.00303	0.01376	642.763593	4.289	3.6	1725 ± 10
1010	642.533	0.0088	0.00117	0.01427	649.662003	5.116	4.3	1737 ± 10
1040	652.668	0.00909	0.00291	0.01543	659.836641	5.832	4.9	1754 ± 10
1110	673.178	0.00599	0.00163	0.01265	681.314380	20.877	17.7	1790 ± 10
1400	682.472	0.0139	0.00117	0.01675	688.831209	19.647	16.7	1803 ± 10

Table 2 (*Continued*)

T (°C)	($^{40}Ar/^{39}Ar$) m	($^{36}Ar/^{39}Ar$) m	($^{37}Ar/^{39}Ar$) m	($^{38}Ar/^{39}Ar$) m	$^{40}Ar^*/^{39}Ar$	^{39}Ar ($\times10^{-12}$ mol)	^{39}Ar/%	Age/Ma (±1sd Ma)
Sample Qu077 (Xueling ductile shear zone, N37°17′53″, E111°17′14″)								
Muscovite								
Plateau age = 1813 ± 12, total gas age = 1809 ± 12 Ma								
750	860.26658	0.01301	10.00288	–	–	–	12.35	1783 ± 12
800	881.05246	0.01303	11.90151	–	–	–	11.84	1812 ± 12
850	880.08206	0.01230	11.33156	–	–	–	9.02	1811 ± 12
900	890.92369	0.01297	12.94337	–	–	–	7.99	1826 ± 12
950	877.02047	0.01159	9.88266	–	–	–	8.66	1806 ± 12
1000	876.22561	0.01374	12.15514	–	–	–	10.40	1806 ± 12
1050	885.66963	0.00967	8.35984	–	–	–	5.94	1816 ± 12
1100	883.96437	0.01108	11.31239	–	–	–	7.04	1816 ± 12
1150	884.32429	0.01152	10.18783	–	–	–	11.48	1815 ± 12
1200	892.24585	0.01021	7.68614	–	–	–	7.62	1824 ± 12
1250	872.60513	0.00903	10.11058	–	–	–	7.56	1801 ± 12
1450	888.66586	0.04846	45.75164	–	–	–	0.10	1844 ± 89

There might be some Ar loss in the lower temperature steps, but the biotite grain gives a total gas age of 1837 ± 15 Ma and a plateau age of 1885 ± 20 Ma for 50% of argon released (steps 9–13) (Fig. 14b).

Rock sample NOR24-2 is a granitic mylonite taken from ~5 km south of Shawanzi (GPS coordinates: N40°54′14.6″/E110°4′16.4″) and consisting of biotite (5%), K-feldspar (20%), plagioclase (35%) and quartz (40%). Polycrystalline quartz ribbons are composed of oriented rectangle quartz grains and extend stably with straight boundaries. Biotites are oriented along polycrystalline quartz ribbons and were not altered. The feldspar fishes included in the quartz ribbons indicate dextral shearing (Fig. 7a). A biotite grain gives a $^{40}Ar/^{39}Ar$ total gas age of 1735 ± 11 Ma, and a plateau age of 1814 ± 13 Ma for 78% of argon released from steps 4 to 13 (Fig. 14c).

(2) *Zongbieli ductile shear zone on the west margin of the Ordos block*. Rock Exc07-1 is a granitic mylonite taken from 8 km northeast of Zongbieli (GPS coordinates: N39°15′53″/E106°10′30″), which consists of quartz (30%), K-feldspar (40%), plagioclase (15%) and biotite (15%) (Fig. 14d). A muscovite grain gives a $^{40}Ar/^{39}Ar$ total gas age of 1739 ± 9 Ma.

(3) *Xueling ductile shear zone on the east margin of the Ordos block*. Rock Qu077 is a granitic mylonite sampled ~2 km west of Xueling (GPS coordinates: N37°18′19″/E111°16′45″), which consists of quartz (40%), K-feldspar (20%), plagioclase (35%) and biotite (5%). The muscovite grain gives a plateau age of 1813 ± 12 Ma for more than 90% of argon released (Fig. 14e).

6. Discussion

6.1. Characteristics of the ductile shear zones on the northern, northwestern and eastern edges of the Ordos block

The ductile shear zones developed at different locations at the margins of the Ordos block have different geometries and kinematic characteristics. On the north margin of the Ordos block, the Wulashan-Daqingshan ductile shear zone is characterized by steeply E-W-trending shearing foliations and subhorizontal E- or W-plunging stretching lineations showing dextral strike-slip ductile shearing. On the west margin of the Ordos block, the Zongbieli ductile shear zone is characterized by NEE-trending medium- to high-angle shearing foliations and medium-angle, SE-plunging stretching lineations showing top-to-the-NW thrusting. On the east margin of the Ordos block, the Xueling ductile shear zone is characterized by NE-SW trending, NW-dipping, medium-angle shearing foliations and medium-angle, NW-plunging stretching lineations. These are kinematic indicators showing top-to-the-SE thrusting accompanied by a sinistral shearing component, which is consistent with the NE-trending ductile shear zones in the central part of the NCC, e.g., the Taihang Suture, Longquanguan thrust and Upper Wutai thrust developed in the Zanhuang, Fuping and Wutai massifs, respectively (Trap et al., 2007, 2008, 2009a,b, 2011, 2012). All of these ductile shear zones are characterized by top-to-the-SE thrusting kinematics. To the north, all the ductile shear zones might be NE-NEE trending, the kinematics of which might be sinistral strike-slip shearing accompanied with top-to-the-NW thrusting, which is consistent with the Zhujiafang ductile shear zone. The E-W trending Zhujiafang ductile shear zone separates the Hengshan massif into northern and southern domains and is characterized by sinistral strike-slip shearing kinematics (Li et al., 2010; Trap et al., 2012).

6.2. Deformation ages of the ductile shear zones on the northern, northwestern and eastern edges of the Ordos block

The ductile shear zones are adjacent to the Ordos block, but whether they are related depends on the formation ages. We carried out ^{40}Ar–^{39}Ar dating of deformed minerals from deformed rocks and LA-ICP-MS U–Pb dating of zircons from anatectic granite in the ductile shear zones.

Three ^{40}Ar–^{39}Ar ages of 1885 ± 20 Ma (NOR14-1), 1841 ± 14 Ma (NOR8-3) and 1814 ± 13 Ma (NOR24-2) were obtained from deformed biotites along the Wulashan-Daqingshan ductile shear zone. A ^{40}Ar–^{39}Ar total age of 1739 ± 9 Ma was obtained from deformed muscovite along the Zongbieli ductile shear zone. One ^{40}Ar–^{39}Ar plateau age of 1813 ± 12 Ma was obtained from deformed muscovite along the Xueling ductile shear zone. The ^{40}Ar–^{39}Ar dating results show that the Wulashan-Daqingshan ductile shear zone initially deformed at 1.88 Ga and continued to 1.81 Ga, while the Xueling ductile shear zones deformed at approximately 1.81 Ga. Trap et al. (2007, 2008, 2009a,b, 2011, 2012) obtained a number of similar ^{40}Ar–^{39}Ar ages of 1.81 Ga, which represent the ages of deformation recorded in the Zhujiafang ductile shear zone, Taihang Suture, Longquanguan thrust and Upper Wutai thrust (Fig. 15).

The ^{40}Ar–^{39}Ar age records the cooling time of the tectonothermal events. Previous studies indicate that the NCC experienced extensive HP and HT-UHT metamorphism during the Paleoproterozoic (approximately 1.95–1.85 Ga). Therefore, the problem of whether the ^{40}Ar–^{39}Ar ages of deformed minerals represent the deformation time of the ductile shear zones or record the natural cooling process of high-grade metamorphism must be considered. To reconstruct the cooling history of the high-grade metamorphic rocks, we obtained a number of metamorphic ages from various high-grade metamorphic rocks on the north and east margins of the Ordos block. These include the SHRIMP and LA-ICP-MS microanalysis dating ages on metamorphic zircon, the EMPA Th–U–Pb dating ages on metamorphic monazite and the ^{40}Ar–^{39}Ar ages of deformed minerals. We analyzed the isotopic ages of different minerals and their corresponding closure temperatures, in addition to the P-T conditions of metamorphism (Fig. 16).

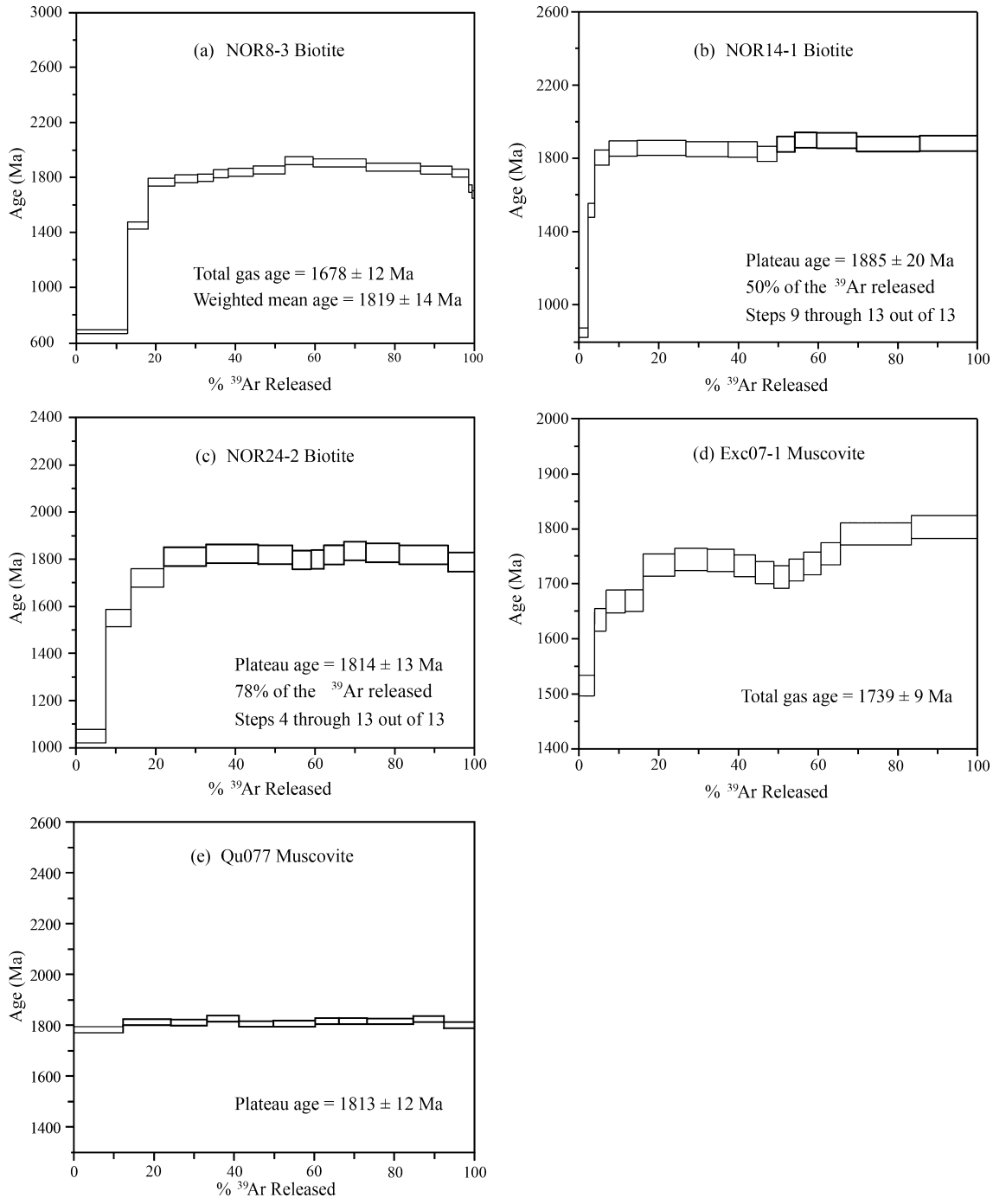

Fig. 14. ^{40}Ar–^{39}Ar age spectra calculated at 2σ.

On the north margin, the khondalitic rocks were deposited at 2.5–2.1 Ga (Wan et al., 2006; Zhai, 2009; Dong et al., 2013a,b) and experienced peak HT-UHT metamorphism and retrograde metamorphism at 1.93–1.90 Ga and 1.89–1.82 Ga, respectively (Wan et al., 2006, 2013b; Santosh et al., 2007a,b; Yin et al., 2009, 2011; Dong et al., 2013a,b; Zhai, 2009; Zhai et al., 2010).

Ultra-high-temperature (UHT) granulites were discovered in Dongpo and Tuguiwula (Guo et al., 2006; Santosh et al., 2006, 2007a,b, 2009a,b), which occurred at ~1.92 Ga (Santosh et al., 2007b). The diagnostic UHT mineral assemblages include sapphirine + quartz and high temperature mesoperthite, with estimated P-T conditions of approximately 1.0 GPa and >1050 °C (Santosh et al., 2012), or a temperature range of 910–980 °C (Guo et al., 2012). These high-grade metamorphic rocks underwent amphibolite facies retrograde metamorphism at 1.85 Ga, with estimated P-T conditions of approximately 650 °C. Given the closure temperature of zircon in the U–Th–Pb system of approximately 900 °C (Lee et al., 1997; Cherniak and Watson, 2000) and the geothermal gradient of 25 °C/km, the high-grade metamorphic rocks were buried at depths greater than approximately 25 km at 1.85 Ga (Fig. 16a).

As previously mentioned, deformed biotites from the high-grade metamorphic rocks of the Wulashan-Daqingshan area give ^{40}Ar–^{39}Ar ages of 1885 ± 20 Ma, 1841 ± 14 Ma and 1814 ± 13 Ma. Given the geothermal gradient of 25 °C/km and the closure temperature in the K-Ar biotite system of approximately 320 °C (Harrison

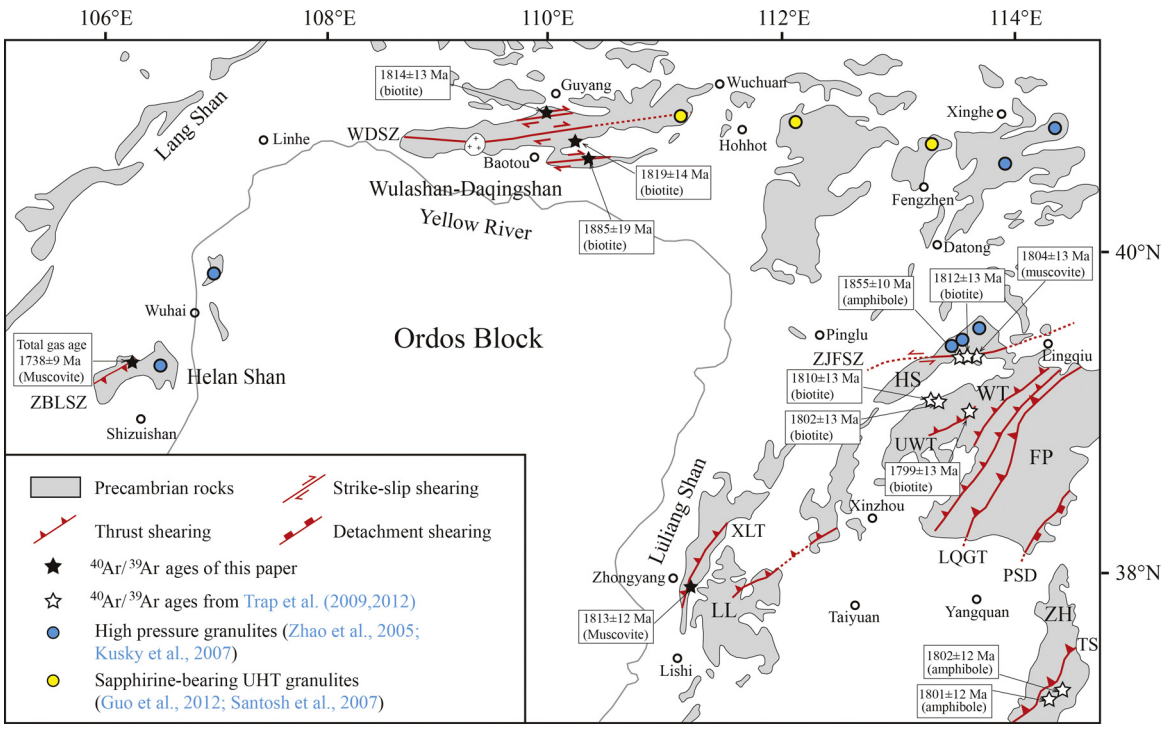

Fig. 15. Major Paleoproterozoic structures and $^{40}Ar/^{39}Ar$ dating results of the west part of the NCC (modified from Kusky et al., 2007). *Abbreviations*: ZBLSZ, Helanshan-Zongbieli shear zone; WDSZ, Wulashan-Daqingshan shear zone; ZSZ, Zhujiafang shear zone; UWT, Upper Wutai thrust; LQGT, Longquanguan thrust; XLT, Lüliangshan-Xueling thrust; TS, Taihang suture; HS, Hengshan massif; WT, Wutai massif; FP, Fuping massif; LL, Lüliang massif; ZH, Zanhuang massif.

et al., 1985), the high-grade metamorphic rocks had been uplifted to the closure temperature of muscovite and biotite, approximately 12–14 km beneath the Earth's surface from 1.89 to 1.81 Ga (Fig. 16).

Liu et al. (2007) proposed that the P-T condition of the Wulashan-Daqingshan ductile shear zone is similar to amphibolite-granulite facies metamorphism, according to the syn-tectonic mineral assemblages (hornblende + plagioclase + clinopyroxene, and hypersthenes along hornblende) in the ductile shear zone. The temperature of hornblende-plagioclase is approximately 575–695 °C, which is similar to the temperature of retrograde metamorphism at 1.85 Ga (Zhai and Santosh, 2011) and is the formation temperature of subvertical foliations (Liu et al., 2007). Previous studies indicate that the granulites experienced strong deformation when they were uplifted to the condition of amphibolite facies.

On the east margin in the central part of the NCC, nearly all metamorphic zircons and monazites yielded consistent metamorphism

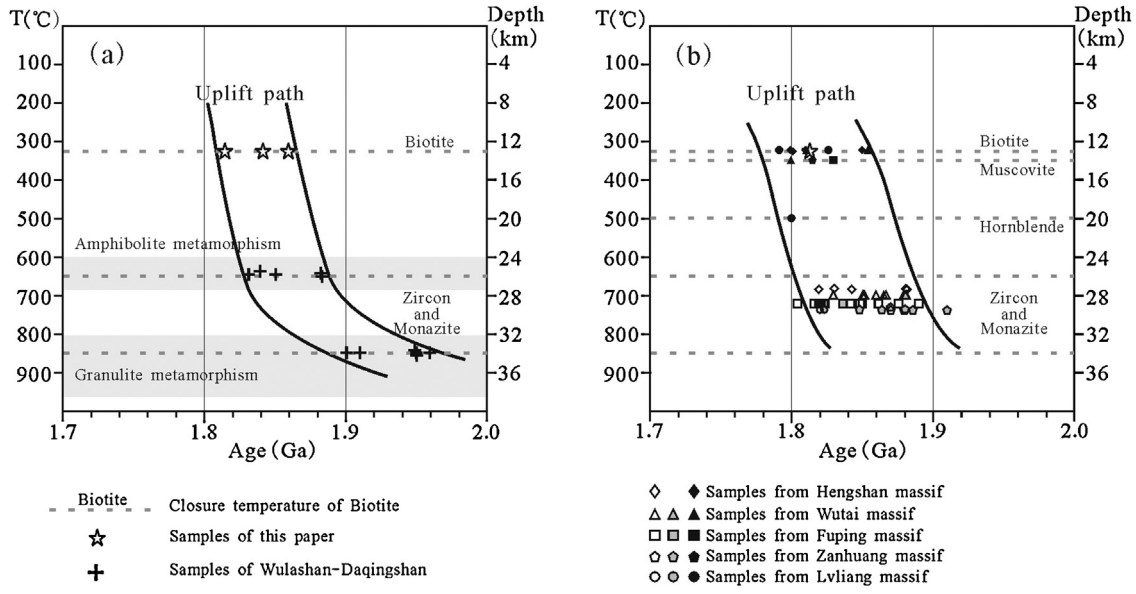

Fig. 16. Uplift-path of high-grade metamorphic rocks according to the closure temperature of different minerals and their corresponding ages (given the geothermal gradient of 25 °C/km). (a) The uplift of high-grade metamorphic rocks in the Wulashan-Daqingshan area, north margin of the Ordos block. Meta-zircon ages are from Xia et al. (2006a), Wan et al. (2009) and Dong et al. (2013a,b). (b) Uplifting of the high-grade metamorphic rocks in the Central part of the NCC, east of the Ordos block. Meta-zircon ages (symbols filled with white color), meta-monazite ages (symbols filled with gray color) and ^{40}Ar–^{39}Ar ages (symbols filled with black color) are from Zhao and Zhai (2013) and references wherein.

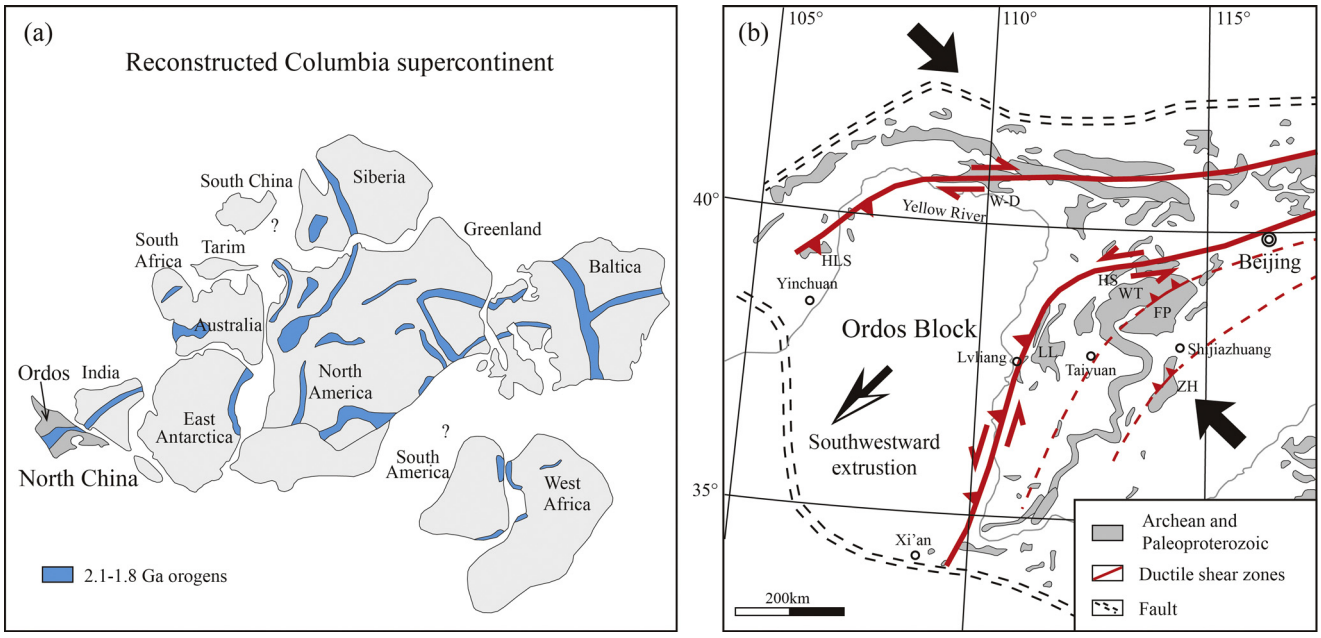

Fig. 17. (a) Reconstructed Columbia supercontinent shows that the south margin of the Ordos block was an open boundary (modified from Zhao et al., 2009). (b) Possible southwestward extrusion of the Ordos Block of the NCC during Paleoproterozoic. *Abbreviations*: HLS, Helanshan; W-D, Wulashan-Daqingshan; HS, Hengshan massif; WT, Wutai massif; FP, Fuping massif; LL, Lüliang massif; ZH, Zanhuang massif.

ages of approximately 1.85 Ga in the Hengshan-Wutaishan-Fuping-Zanhuang-Lüliang massifs (Zhao and Zhai, 2013 and references therein), which indicates that the massifs were still in the condition of the closure temperatures of zircon and monazite at this time. The massifs were buried at depths exceeding 25 km, given the closure temperature of zircon and monazite of approximately 900 °C (Lee et al., 1997; Cherniak and Watson, 2000) and 700–800 °C (Suzuki et al., 1994; Spear and Parrish, 1996; Kalt et al., 2000), respectively, and the geothermal gradient of approximately 25 °C/km (Fig. 16a).

As previously mentioned, we obtained a muscovite ^{40}Ar–^{39}Ar age of 1813 ± 12 Ma from the Xueling ductile shear zone in the Lüliang massif (Fig. 16a). Trap et al. (2008, 2012) and Wang et al. (2003) obtained a number of ^{40}Ar–^{39}Ar ages for biotite and muscovite from the Hengshan-Wutai-Fuping-Zanhuang-Lüliang massifs; most of the ages concentrated approximately 1810 Ma (Fig. 16b). Given the geothermal gradient of approximately 25 °C/km and the closure temperature of muscovite and biotite in the K-Ar system of approximately 350 °C (Hurford et al., 1991) and 320 °C, respectively, the high-grade metamorphic rocks were uplifted to a depth of approximately 12–14 km below the surface until 1.80–1.81 Ga (Fig. 16b).

The analyses of the closure temperatures and the corresponding dating results for different minerals indicate that the high-grade metamorphic rocks in the north and east margin of the Ordos block experienced fast cooling (approximately 300 °C) and strong uplifting (exceeding 10 km) ~1.85–1.80 Ga after peak metamorphic conditions were reached. This is in agreement with previous studies (Trap et al., 2007; Zhai and Santosh, 2011). Zhai and Santosh (2011) proposed that the HP and HT-UHT granulites underwent a rapid exhumation from the lowermost-lower to lower-middle crust level in the Daqingshan area located on the north margin of the Ordos block. Trap et al. (2007) suggested that uplift and doming of the cratonic basement occurred in the latest Paleoproterozoic according to the age difference (up to 500–700 Ma) between the sedimentary cover and the metamorphic basement in the Hengshan-Wutai-Fuping area located on east margin of the Ordos block.

The fast cooling and strong uplifting of the high-grade metamorphic rocks from 1.85 to 1.80 Ga might have resulted from the extensively developed ductile shearing deformation on the northern, northwestern and eastern edges of the Ordos block. Therefore, the deformation ages of the ductile shear zones could be constrained by the ^{40}Ar–^{39}Ar ages of the deformed minerals. For the Zongbieli ductile shear zone, only a total ^{40}Ar–^{39}Ar gas age of 1739 ± 9 Ma was obtained, which is inconsistent with the other dates and may not represent the real deformation age. Yin et al. (2011) obtained a zircon age of ~1.84 Ga from S-type granites, which shows syn-tectonic characteristics (Fig. 8) and can represent the deformation age of the Zongbieli ductile shear zone. Similarly, the zircon U–Pb age of 1858 ± 21 Ma from syn-tectonic granite in the Wulashan-Daqingshan area represents the deformation age of the ductile shear zone. The ^{40}Ar–^{39}Ar ages of deformed minerals and the zircon U–Pb ages indicate that the deformation age of the ductile shear zones on the northern, northwestern and eastern edges of the Ordos block is approximately 1.85–1.80 Ga.

6.3. Possible Paleoproterozoic southwestward extrusion of the Ordos Block

Although the kinematics of the ductile shear zones differ on the northern, northwestern and eastern edges of the Ordos block, the similar age of deformation indicates that they might be genetically correlated. We postulated that the Ordos block moved to the southwest direction in the late Paleoproterozoic approximately 1.85–1.81 Ga according to the geometry, kinematic and geochronology characteristics of the surrounding ductile shear zones. The Wulashan-Daqingshan and Zongbieli ductile shear zones consist of the northwest boundary of the Ordos block, which extends to the east along the ultra-high-temperature metamorphic belt. The Zhujiafang and Xueling ductile shear zones consist of the southeast boundary of the Ordos block (Figs. 15 and 17). The southwest margin of the Ordos block might have been an open boundary at this time according to the following evidences. Firstly, the NCC was located in the margin of the Supercontinent and there is no continents existed on the southern margin of it according to Paleomagnetic reconstructions of the Columbia supercontinent (Zhao et al., 2009; Xia et al., 2013, and references therein) (Fig. 17a). Secondly, petrological, geochemical and geochronological studies suggested that the Xiong'er volcanic rocks developed along the

southern margin of the NCC is formed in an Andean-type continental margin arc and most likely to have resulted from the outgrowths of the Columbia supercontinent (Zhao et al., 2002b, 2003b; He et al., 2008, 2009, 2010), which means that the southern margin of the NCC must have faced an open ocean before about 1.78 Ga (He et al., 2008, 2009, 2010). Thirdly, the Qinling orogen separating the North and South China blocks was built up through the middle Paleozoic and Late Triassic collision (Meng and Zhang, 2000). It is hard to estimate the distance of extrusion at present. To the southwest, thrusting is the main deformation form, and which resulted in the uplift of the Ordos block. The possible southwestward extrusion of the Ordos block might have resulted from the westward subduction of the Eastern Block under the Western Block, which collided along Trans-North China Orogen at approximately 1.85 Ga, and the collision of the NCC with part (South America?) of the Columbia supercontinent (Kusky et al., 2007).

The possible southwestward extrusion of the Ordos block defined by the peripheral ductile shear zones indicates that the structural process of the North China Craton was complicated.

7. Conclusions

(1) Ductile shear zones with differing kinematics developed on different margins of the Ordos block. On the north margin, the Wulashan-Daqingshan ductile shear zone shows dextral strike-slip shearing kinematics. On the west margin, the Zongbieli ductile shear zone shows top-to-the-NW thrusting. On the east margin, the Xueling ductile shear zone shows top-to-the-SE thrusting kinematics accompanied by a sinistral strike-slip shearing component.
(2) The ductile shear zones on the northern, northwestern and eastern edges of the Ordos Block have similar deformation ages. The zircon U–Pb ages of syn-tectonic anatectic granite veins show that the deformation began at approximately 1.85 Ga and continued to approximately 1.81 Ga, according to the ^{40}Ar–^{39}Ar ages of deformed minerals.
(3) The similar deformation ages indicate that the ductile shear zones might be genetically correlated. The geometry and kinematics of the ductile shear zones defined the possible southwestward extrusion of the Ordos block in the late Paleoproterozoic approximately 1.85–1.81 Ga, which might be correlated to the amalgamation of the Columbia supercontinent.

Acknowledgments

We thank Qingren Meng and Shuanhong Zhang for useful discussions and helpful suggestions. Comments from two anonymous reviewers and the journal editor have greatly improved the manuscript. We also thank Minghua Ren and Kathleen Zanetti from the $^{40}Ar/^{39}Ar$ Lab of the University of Nevada, Las Vegas, America and Jianzhen Geng from the MC-LA-ICP-MS Lab of the Tianjin Institute of Geology and Mineral Resources, Tianjin, China. This research was funded by the National Basic Research Program of China (2012CB416604), the National Natural Science Foundation of China (91114204) and the Geological Investigation Project of China Geological Survey (1212011220259).

References

BGMRNP (Bureau of Geology and Mineral Resources of the Ningxia Province), 1991. Regional Geological Survey of Xi'an Geosciences University, Hulusitai sheet (J-48-33-A), scale 1:50,000 (in Chinese).
BGMRSP (Bureau of Geology and Mineral Resources of the Shanxi Province), 1976. Fenyang sheet (J-49-XXVIII), scale 1:200,000 (in Chinese).
BGMRIMP (Bureau of Geology and Mineral Resources of the Inner Mongolia Province), 1971. Shetaizhen sheet (K-49-XXVI), scale 1:200, 000 (in Chinese).
Black, L.P., Kamo, S.L., Allen, C.M., Aleinikoff, J.N., Davis, D.W., Kosch, R.J., Foudoulis, C., 2003. TEMORA 1: a new zircon standard for Phanerozoic U–Pb geochronology. Chem. Geol. 200, 155–170.
Bochez, J., 1977. Plastic deformation of quartites at lower temperature in an area of natural strain gradient. Tectonophysics 39, 25–50.
CESJU (College of Earth Science, Jilin University), 2003. Baotou sheet (K49C004002), scale 1:200,000 (in Chinese).
Chen, X.F., Liu, Z.H., Xu, Z.Y., Zhao, Q.Y., Wu, X.W., 2008. The characters and genesis of the lower crust Daqingshan ductile shear zones in the Inner Mongolia. J. Mineral. Petrol. 1, 48–53 (in Chinese with English abstract).
Cherniak, D.J., Watson, E.B., 2000. Pb diffusion in zircon. Chem. Geol. 172, 5–24.
Condie, K.C., Boryta, M.D., Liu, J.Z., Qian, X.L., 1992. The origin of khondalites: geochemical evidence from the Archean to Early Proterozoic granulite belt in the North China Craton. Precambrian Res. 59, 207–223.
Diwu, C.R., Sun, Y., Simon, A.W., Wang, H.L., Dong, Z.C., Zhang, H., Wang, Q., 2013. New evidence for ~4.45 Ga terrestrial crust from zircon xenocrysts in Ordovician ignimbrite in the North Qinling Orogenic Belt, China. Gondwana Res. 23, 1484–1490.
Dong, C.Y., Wan, Y.S., Xu, Z.Y., Liu, D.Y., Yang, Z.S., Ma, M.Z., Xie, H.Q., 2012. Khondalites of the late Paleoproterozoic in the Daqingshan area, North China Craton: SHRIMP zircon U–Pb dating. Sci. China Earth Sci. 56, 115–125.
Dong, C.Y., Wan, Y.S., Simon, A.W., Xu, Z.Y., Ma, M.Z., Xie, H.Q., Liu, D.Y., 2013a. Earliest Paleoproterozoic supracrust rocks in the North China Craton recognized from the Daqingshan area of the Khondalite Belt: constraints on craton evolution. Gondwana Res., http://dx.doi.org/10.1016/j/gr.2013.05.021.
Dong, C.Y., Wan, Y.S., Xu, Z.Y., Liu, D.Y., Yang, Z.S., Ma, M.Z., Xie, H.Q., 2013b. SHRIMP zircon U–Pb dating of late Paleoproterozoic khondalites in the Daqing Mountains area on the North China Craton. Sci. China Earth Sci. 1, 115–125.
Faure, M., Trap, P., Lin, W., Monie, P., Bruguier, O., 2007. Polyorogenic evolution of the Paleoproterozoic Trans-North China Belt, new insights from the Lüliangshan-Hengshan-Wutaishan and Fuping massifs. Episodes 30, 1–12.
Geng, Y.S., Wan, Y.S., Shen, Q.H., Li, H.M., Zhang, R.X., 2000. Chronological framework of the early Precambrian important events in the Lüliang area, Shanxi Province. Acta Geol. Sin. 74, 216–223 (in Chinese with English abstract).
Geng, Y.S., Wan, Y.S., Yang, C.H., 2003. The Paleoproterozoic rift-type volcanism in Lüliangshan Area, Shanxi Province, and its geological significance. Acta Geosci. Sin. 24, 97–104 (in Chinese with English abstract).
Geng, Y.S., Yang, C.H., Song, B., Wan, Y.S., 2004. Post-orogenic granites with an age of 1800 Ma in Lüliang area, North China Craton: constraints from isotopic geochronology and geochemistry. Geol. J. Chin. Univ. 10, 477–487 (in Chinese with English abstract).
Guo, J.H., Chen, Y., Peng, P., Liu, F., Chen, L., Zhang, L.Q., 2006. Sapphrine granulite from Daqingshan area, Inner Mongolia ~1.85 Ga ultrahigh temperature (UHT) metamorphism. In: Proceedings of National Conference on Petrology and Geodynamics in China (Nanjing), pp. 215–218.
Guo, J.H., Peng, P., Chen, Y., Jiao, S.J., Windley, B.F., 2012. UHT sapphirine granulite metamorphism at 1.93–1.92 Ga caused by gabbronorite intrusions: implications for tectonic evolution of the northern margin of the North China Craton. Precambrian Res. 222–223, 124–142.
Harrison, T.M., Duncan, I., McDougall, I., 1985. Diffusion of ^{40}Ar in biotite: temperature, pressure and compositional effects. Geochem. Cosmochim. Acta 49, 2461–2468.
He, Y.H., Zhao, G.C., Sun, M., Wilde, S.A., 2008. Geochemistry, isotope systematic and petrogenesis of the volcanic rocks in the Zhongtiao Mountain: an alternative interpretation for the evolution of the southern margin of the North China Craton. Lithos 102, 158–178.
He, Y.H., Zhao, G.C., Sun, M., Xia, X.P., 2009. SHRIMP and LA-ICP-MS zircon geochronology of the Xiong'er volcanic rocks: implications for the Paleoproterozoic evolution of the southern margin of the North China Craton. Precambrian Res. 168, 213–222.
He, Y.H., Zhao, G.C., Sun, M., Han, Y.G., 2010. Petrogenesis and tectonic setting of volcanic rocks in the Xiaoshan and Waifangshan areas along the southern margin of the North China Craton: constraints from bulk-rock geochemistry and Sr–Nd isotopic composition. Lithos 114, 186–199.
Hippertt, J., Rocha, A., Lana, C., Silva, E., Takeshita, T., 2001. Quartz plastic segregation and ribbon in high-grade striped gneisses. J. Struct. Geol. 23, 67–80.
Hu, J.M., Liu, X.S., Li, Z.H., Zhao, Y., Zhang, S.H., Liu, X.C., Qu, H.J., Chen, H., 2013. SHRIMP U–Pb zircon dating of the Ordos Basin basement and its tectonic significance. Chin. Sci. Bull. 58, 118–127.
Hurford, A.J., Hunziker, J.C., Stockhert, B., 1991. Constraints on the late thermotectonic evolution of the western Alps: evidence for episodic rapid uplift. Tectonics 4, 758–769.
Isik, V., 2009. The ductile shear zone in granitoid of the Central Anatolian Crystalline Complex, Turkey: implications for the origins of the Tuzgolu basin during the Late Cretaceous extensional deformation. J. Asian Earth Sci. 34, 507–521.
Jackson, S.E., Pearson, N.J., Griffin, W.L., Belousova, E.A., 2004. The application of laser ablation-inductively coupled plasma-mass spectrometry to in situ U–Pb zircon geochronology. Chem. Geol. 211, 47–69.
Justet, L., Spell, T.L., 2001. Effusive eruptions from a large shallow magma chamber: the Bearhear Rhyolite, Jemez Volcanic Field, New Mexico. J. Volcanol. Geotherm. Res. 107, 241–264.
Kalt, A., Corfu, F., Wijbrans, J.R., 2000. Time calibration of a P-T path from a Variscan high-temperature low-pressure metamorphic complex (Bayerische Wald, Germany) and the detection of inherited monazite. Contrib. Mineral. Petrol. 138, 143–163.

Kröner, A., Wilde, S.A., Li, J.H., Wang, K.Y., Zhao, G.C., 2005. Age and evolution of a late Archean to early Palaeozoic upper to lower crustal section in the Wutaishan/Hengshan/Fuping terrain of north China. J. Asian Earth Sci. 24, 577–595.
Kusky, T.M., Li, J.H., 2003. Paleoproterozoic tectonic evolution of the North China Craton. J. Asian Earth Sci. 22, 23–40.
Kusky, T.M., Li, J.H., Santosh, M., 2007. The Paleoproterozoic North Hebei Orogen: North China Craton's collisional suture with the Columbia supercontinent. Gondwana Res. 12, 4–28.
Lee, J., Williams, Ellis, D., 1997. Pb, U and Th diffusion in nature zircon. Nature 13, 159–162.
Li, S.Z., Zhao, G.C., Sun, M., Han, Z.Z., Hao, D.F., Luo, Y., Xia, X.P., 2005. Deformation history of the Paleoproterozoic Liaohe Group in the Eastern Block of the North China Craton. J. Asian Earth Sci. 24, 659–674.
Li, S.Z., Zhao, G.C., Sun, M., Luo, Y., Han, Z.Z., Zhao, G.T., 2006. Are the South and North Liaohe Groups different exotic terranes? Nd isotope constraints on the Jiao-Liao-Ji orogen. Gondwana Res. 9, 198–208.
Li, S.Z., Zhao, G.C., 2007. SHRIMP U–Pb zircon geochronology of the Liaoji Granitoids: constraints on the Paleoproterozoic Jiao-Liao-Ji belt in the eastern block of the North China craton. Precambrian Res. 158, 1–16.
Li, S.Z., Zhao, G.C., Zhang, J., Sun, M., Zhang, G.W., Dai, L.M., 2010. Deformation history of the Hengshan-Wutai-Fuping complexes: implications for the evolution of the Trans-North China Orogen. Gondwana Res. 18, 611–631.
Li, S.Z., Zhao, G.C., Santosh, M., Liu, X., Dai, L.M., 2011a. Paleoproterozoic tectonothermal evolution and deep crustal processes in the Jiao-Liao-Ji Belt, North China Craton: a review. Geol. J. 46, 525–543.
Li, S.Z., Zhao, G.C., Santosh, M., Liu, X., Lai, L.M., Suo, Y.H., Song, M.C., Wang, P.C., 2012. Structural evolution of the Jiaobei Massif in the southern segment of the Jiao-Liao-Ji Belt, North China Craton. Precambrian Res. 200–203, 59–73.
Li, X.P., Yang, Z.Y., Zhao, G.C., Grapes, R., Guo, J.H., 2011b. Geochronology of khondalite series rocks of the Jining Complex: confirmation of depositional age and tectonometamorphic evolution of the North China craton. Int. Geol. Rev. 53, 1194–1211.
Liu, S.W., Zhao, G.C., Wilde, S.A., Shu, G.M., Sun, M., Li, Q.G., Tian, W., Zhang, J., 2006. Th–U–Pb monazite geochronology of the Lüliang and Wutai Complexes: constraints on the tectonothermal evolution of the Trans-North China Orogen. Precambrian Res. 148, 205–224.
Liu, Z.H., Xu, Z.Y., Wang, K.Y., 2007. Evidence of microstructures and fluid inclusions for the origin of polycrystalline quartz ribbons in high-grade metamorphic rocks in Daqingshan region. Sci. China Earth Sci. 4, 496–504.
Liu, Y.S., Gao, S., Hu, Z.C., Gao, C.G., Zong, K.Q., Wang, D.B., 2009. Continental and oceanic crust recycling-induced melt-peridotite interactions in the Trans-North China Orogen: U–Pb dating, Hf isotopes and trace elements in zircons from mantle xenoliths. J. Petrol. 1–2, 537–571.
Liu, Y.S., Hu, Z.C., Zong, K.Q., Gao, C.G., Gao, S., Xu, J., Chen, H.H., 2010. Reappraisement and refinement of zircon U–Pb isotope and trace element analyses by LA-ICP-MS. Sci. China Earth Sci. 15, 1535–1546.
Ludwig, K.R., 2003. User's Manual for Isoplot/Ex, version 3.00. A Geochronological Toolkit for Microsoft Exel. Berkeley Geochronology Center Special Publication No. 4, pp. 1–70.
Ma, M.Z., Wan, Y.S., Santosh, M., Xu, Z.Y., Xie, H.Q., Dong, C.Y., Liu, D.Y., 2012. Decoding multiple tectono-thermal events in zircons from single rock samples: SHRIMP zircon U–Pb data from the late Neoarchean rocks of Daqingshan, North China Craton. Gondwana Res. 22, 810–827.
Meng, Q.R., Zhang, G.W., 2000. Geological framework and tectonic evolution of the Qinling orogen, central China. Tectonophysics 323, 183–196.
Miao, L.C., Qiu, Y.M., Guan, K., Naughton, N.M., Qiu, Y.S., Luo, Z.K., David, G., 2001. A chronological study of SHRIMP U–Pb of zircon from the Dahuabei Intrusion in the Wulashan area, Inner Mongolia. Geol. Rev. 47, 169–174 (In Chinese with English abstract).
Santosh, M., Sajeev, K., Li, J.H., 2006. Extreme crustal metamorphism during Columbia supercontinent assembly: evidence from North China Craton. Gondwana Res. 10, 256–266.
Santosh, M., Tsunogae, T., Li, J.H., Liu, S.J., 2007a. Discovery of sapphirine-bearing Mg–Al granulites in the North China Craton: implications for Paleoproterozoic ultrahigh-temperature metamorphism. Gondwana Res. 11, 263–285.
Santosh, M., Wilde, S., Li, J.H., 2007b. Timing of Paleoproterozoic ultrahigh temperature metamorphism in the North China Craton: evidence from SHRIMP U–Pb zircon geochronology. Precambrian Res. 159, 178–196.
Santosh, M., Tsunogae, T., Ohyama, H., Sato, K., Li, J.H., Liu, S.J., 2008. Carbonic metamorphism at ultrahigh-temperatures: evidence from North China Craton. Earth Planet. Sci. Lett. 266, 149–165.
Santosh, M., Maruyama, S., Yamamoto, S., 2009a. The making and breaking of supercontinents: some speculations based on superplumes, superdownwelling and the role of tectosphere. Gondwana Res. 15, 324–341.
Santosh, M., Sajeev, K., Li, J.H., Liu, S.J., Itaya, T., 2009b. Counterclockwise exhumation of a hot orogen: the Paleoproterozoic ultrahigh-temperature granulites in the North China Craton. Lithos 110, 140–152.
Santosh, M., Wan, Y., Liu, D., Chunyan, D., Li, J., 2009c. Anatomy of zircons from an ultrahot Orogen: the amalgamation of North China Craton within the supercontinent Columbia. J. Geol. 117, 429–443.
Santosh, M., Zhao, D.P., Kusky, T., 2010. Mantle kinematics of the Paleoproterozoic North China Craton: a perspective based on seismic tomography. J. Geokinem. 49, 39–53.
Santosh, M., Liu, S.J., Tsunogae, T., Li, J.H., 2012. Paleoproterozoic ultrahigh-temperature granulites in the North China Craton: implications for tectonic models on extreme crustal metamorphism. Precambrian Res. 222–223, 77–106.
Spear, F.S., Parrish, R.R., 1996. Petrology and cooling rates of the Valhalla complex, British Columbia, Canada. J. Petrol. 37, 733–765.
Spell, T.L., McDougall, I., 2003. Characterization and calibration of $^{40}Ar/^{39}Ar$ dating standards. Chem. Geol. 198, 189–211.
Staudacher, T., Jessberger, E.K., Dörflinger, D., Kiko, J., 1978. A refined ultrahigh-vacuum furnace for rare gas analysis. J. Phys. Sci. Instrum. 11, 781–784.
Suzuki, K., Adachi, M., Kajizuka, I., 1994. Electron microprobe observations of Pb diffusion in metamorphosed detrital monazites. Earth Planet. Sci. Lett. 128, 391–405.
Tam, P.Y., Zhao, G.C., Sun, M., Li, S.Z., Iizuka, Y., Ma, G.S., Yin, C.Q., He, Y.H., Wu, M.L., 2012a. Metamorphic P-T path and tectonic implications of medium-pressure politic granulites from the Jiaobei massif in the Jiao-Liao-Ji Belt, North China Craton. Precambrian Res. 220–221, 177–191.
Tam, P.Y., Zhao, G.C., Zhou, X.W., Sun, M., Guo, J.H., Li, S.Z., Yin, C.Q., Wu, M.L., He, Y.H., 2012b. Metamorphic P-T path and implications of high-pressure politic granulites from the Jiaobei massif in the Jiao-Liao-Ji Belt, North China Craton. Gondwana Res. 22, 104–117.
Trap, P., Faure, M., Lin, W., Monie, P., 2007. Late Paleoproterozoic (1900–1800 Ma) nappe stacking and polyphase deformation in the Hengshan-Wutaishan area: implications for the understanding of the Trans-North-China Belt, North China Craton. Precambrian Res. 156, 85–106.
Trap, P., Faure, M., Lin, W., Bruguier, O., Monie, P., 2008. Contrasted tectonic styles for the Paleoproterozoic evolution of the North China Craton. Evidence for a ~2.1 Ga thermal and tectonic event in the Fuping Massif. J. Struct. Geol. 30, 1109–1125.
Trap, P., Faure, M., Lin, W., 2009a. The Zanhuang Massif, the second and eastern suture zone of the Paleoproterozoic Trans-North China Orogen. Precambrian Res. 172, 80–98.
Trap, P., Faure, M., Lin, W., Meffre, S., 2009b. The Lüliang Massif: a key area for the understanding of the Paleoproterozoic Trans-North China Belt, North China Craton. Geol. Soc. London Spec. Publ. 323, 99–125.
Trap, P., Faure, M., Lin, W., Augier, R., Fouassier, A., 2011. Syn-collisional channel flow and exhumation of Paleoproterozoic high pressure rocks in the Trans-North China Orogen: the critical role of partial-melting and orogenic bending. Gondwana Res. 20, 498–515.
Trap, P., Faure, M., Lin, W., Breton, N.L., Monie, P., 2012. Paleoproterozoic tectonic evolution of the Trans-North China Orogen: toward a comprehensive model. Precambrian Res. 222–223, 191–211.
Wan, Y.S., Geng, Y.S., Shen, Q.H., Zhang, R., 2000. Khondalite series: geochronology and geochemistry of the Jiehekou Group in Lüliang area, Shanxi province. Acta Petrol. Sin. 16, 49–58.
Wan, Y.S., Song, B., Liu, D.Y., Wilde, S.A., Wu, J.S., Shi, Y.R., Yin, X.Y., Zhou, H.Y., 2006. SHRIMP U–Pb zircon geochronology of Paleoproterozoic metasedimentary rocks in the North China Craton: evidence for a major Late Palaeoproterozoic tectonothermal event. Precambrian Res. 149, 249–271.
Wan, Y.S., Liu, D.Y., Dong, C.Y., Xu, Z.Y., Wang, Z.J., Wilde, S.A., Yang, Y.H., Liu, Z.H., Zhou, H.Y., 2009. The Precambrian Khondalite Belt in the Daqingshan area, North China Craton: evidence for multiple metamorphic events in the Palaeoproterozoic. In: Reddy, S.M., Mazumder, R., Evans, D.A.D., Collins, A.S. (Eds.), Palaeoproterozoic Supercontinents and Global Evolution. Geological Society London, Special Publications, 323, pp. 73–97.
Wan, Y.S., Xie, H.Q., Yang, H., Wang, Z.J., Liu, D.Y., Kroner, A., Wilde, S.A., Geng, Y.S., Sun, L.Y., Ma, M.Z., Liu, S.J., Dong, C.Y., Du, L.L., 2013a. Is the Ordos Block Archean or Paleoproterozoic in age? Implications for the Precambrian evolution of the North China Craton. Am. J. Sci. 313, 683–711.
Wan, Y.S., Xu, Z.Y., Dong, C.Y., Nutman, A., Ma, M.Z., Xie, H.Q., Liu, S.J., Liu, D.Y., Wang, H.C., Cu, H., 2013b. Episodic Paleoproterozoic (~2.45, ~1.95 and ~1.85 Ga) mafic magmatism and associated high temperature metamorphism in the Daqingshan area, North China Craton: SHRIMP zircon U–Pb dating and whole-rock geochemistry. Precambrian Res. 224, 71–93.
Wang, Y.J., Fan, W.M., Zhang, Y., Guo, F., 2003. Structural evolution and $^{40}Ar/^{39}Ar$ dating of the Zanhuang metamorphic domain in the North China Craton: constraints on Paleoproterozoic tectonothermal overprinting. Precambrian Res. 122, 159–182.
Wilde, S.A., Zhao, G.C., Sun, M., 2002. Development of the North China craton during the Late Archean and its final amalgamation at 1.8 Ga: some speculations on its position within a global Palaeoproterozoic supercontinent. Gondwana Res. 5, 85–94.
Wilde, S.A., Zhao, G.C., 2005. Archean to Paleoproterozoic evolution of the North China Craton. J. Asian Earth Sci. 24, 519–522.
Wilde, S.A., Zhao, G.C., Wang, K.Y., Sun, M., 2004. First precise SHRIMP U–Pb zircon ages for the Hutuo Group, Wutaishan: further evidence for the Paleoproterozoic amalgamation of the North China Craton. Sci. China Earth Sci. 49, 83–90.
Wu, M.L., Zhao, G.C., Sun, M., Yin, C.Q., Li, S.Z., Tam, P.Y., 2012. Petrology and P-T path of the Yishui mafic granulites: implications for tectonothermal evolution of the Western Shandong Complex in the Eastern Block of the North China Craton. Precambrian Res. 222–223, 312–324.
Wu, M.L., Zhao, G.C., Sun, M., Li, S.Z., He, Y.H., Bao, Z.A., 2013. Zircon U–Pb geochronology and Hf isotopes of major lithologies from the Yishui Terrane: implications for the crustal evolution of the Eastern Block, North China Craton. Lithos 170–171, 164–178.
Xia, L.Q., Xia, Z.C., Xu, X.Y., Li, X.M., Ma, Z.P., 2013. Late Paleoproterozoic rift-related magmatic rocks in the North China Craton: geological records of rifting in the Columbia supercontinent. Earth Sci. Rev. 125, 69–86.
Xia, X.P., Sun, M., Zhao, G.C., Wu, F.Y., Xu, P., Zhang, J.H., Luo, Y., 2006a. U–Pb and Hf isotopic study of detrital zircons from the Wulashan khondalites: constraints

on the evolution of the Ordos Terrane, Western Block of the North China Craton. Earth Planet. Sci. Lett. 241, 581–593.
Xia, X.P., Sun, M., Zhao, G.C., Luo, Y., 2006b. LA-ICP-MS U–Pb geochronology of detrital zircons from the Jining Complex, North China Craton and its tectonic significance. Precambrian Research 144, 199–212.
Xia, X.P., Sun, M., Zhao, G.C., Wu, F.Y., Xu, P., Zhang, J.S., 2008. Paleoproterozoic crustal growth events in the Western Block of the North China Craton: evidence from detrital zircon Hf and whole rock Sr–Nd isotopes of the khondalites in the Jining Complex. Am. J. Sci. 308, 304–327.
Xia, X.P., Sun, M., Zhao, G.C., Wu, F.Y., Xu, P., Zhang, J.S., 2009. Detrital zircon U–Pb age and Hf isotope study of the khondalite in Trans-North China Orogen and its tectonic significance. Geol. Mag. 146, 701–716.
Yang, Z.S., Xu, Z.Y., Liu, Z.H., 2003. Consideration and practice of the construction of lithostratigraphic system in high-grade metamorphic terrains: a case study in the Daqingshan-Wulashan area. Geol. China 30, 343–351 (in Chinese with English abstract).
Yin, C.Q., Zhao, G.C., Sun, M., Xia, X.P., Wei, C.J., Leung, W.H., 2009. LA-ICP-MS U–Pb zircon ages of the Qianlishan Complex: constrains on the evolution of the Khondalite Belt in the Western Block of the North China Craton. Precambrian Res. 174, 78–94.
Yin, C.Q., Zhao, G.C., Guo, J.H., Sun, M., Xia, X.P., Zhou, X.W., Liu, C.H., 2011. U–Pb and Hf isotopic study of zircons of the Helanshan Complex: constrains on the evolution of the Khondalite Belt in the Western Block of the North China Craton. Lithos 122, 25–38.
Yu, H.F., Sun, D.Y., 1996. Deformational-Metamorphic evolution of ductile shear zone in Daqingshan area. J. Changchun Univ. Earth Sci. 3, 310–315 (in Chinese with English abstract).
Yu, J.H., Wang, C.R., Li, H.M., 1997. Ages of Lüliang group and its metamorphism in Mt. Lüliang Region, Shanxi Province: evidence from single grain zircon U-Pb dating. Chin. J. Geochem. 16, 170–177.
Yu, J.H., Wang, D.Z., 1999. A Paleoproterozoic A-type Rhyolite. Chin. J. Geochem. 18, 219–228.
Zhai, M.G., Peng, P., 2007. Paleoproterozoic events in North China Craton. Acta Petrol. Sin. 23, 2665–2682 (in Chinese with English abstract).
Zhai, M.G., 2009. Two kinds of granulates (HT-HP and HT-UHT) in North China Craton: their genetic relation and geotecotonic implications. Acta Petrol. Sin. 25, 1753–1771.
Zhai, M.G., Li, T.S., Peng, P., Hu, B., Liu, F., Zhang, Y.B., Guo, J.H., 2010. Precambrian key tectonic events and evolution of the North China Craton. In: Kusky, T.M., Zhai, M.G., Xiao, W.J. (Eds.), The Evolving Continents. Geological Society of London, Special Publication 338, pp. 235–262.
Zhai, M.G., Santosh, M., 2011. The early Precambrian odyssey of North China Craton: a synoptic overview. Gondwana Res. 20, 6–25.
Zhai, M.G., 2011. Cratonization and the Ancient North China Continent: a summary and review. Sci. China Earth Sci. 54, 1110–1120.
Zhang, J.S., Driks, P.H., Passchier, C.W., 1994. Extensional collapse and uplift of a polymetamorphic granulite terrain in the Archean of North China. Precambrian Res. 67, 37–57.
Zhang, J., Zhao, G.C., Li, S.Z., Sun, M., Liu, S.W., Simon, A.W., Kroner, A., Yin, C.Q., 2007. Deformation history of the Hengshan Complex: implications for the tectonic evolution of the Trans-North China Orogen. J. Struct. Geol. 29, 933–949.
Zhang, J., Zhao, G.C., Li, S.Z., Sun, M., Liu, S.W., Yin, C.Q., 2009. Deformational history of the Fuping Complex and new U–Th–Pb geochronological constraints: implications for the tectonic evolution of the Trans-North China Orogen. J. Struct. Geol. 31, 177–193.
Zhao, G.C., Wilde, S.A., Cawood, P.A., 1998. Thermal evolution of Archean basement rocks from the eastern part of the North China craton and its bearing on tectonic setting. Int. Geol. Rev. 40, 706–721.
Zhao, G.C., Wilde, S.A., Cawood, P.A., Sun, M., 2001. Archean blocks and their boundaries in the North China Craton: lithological, geochemical, structural and P-T path constrains and tectonic evolution. Precambrian Res. 107, 45–73.
Zhao, G.C., Wilde, S.A., Cawood, P.A., Sun, M., 2002a. SHRIMP U–Pb zircon ages of the Fuping Complex: implications for accretion and assembly of the North China Craton. Am. J. Sci. 302, 191–226.
Zhao, G.C., Cawood, P.A., Wilde, S.A., Sun, M., 2002b. Review of global 2.1–1.8 Ga orogens: implications for a pre-Rodinia supercontinent. Earth Sci. Rev. 59, 125–162.
Zhao, G.C., Sun, Min, Wilde, S.A., 2003a. Major tectonic units of the North China Craton and their Paleoproterozoic assembly. Sci. China Earth Sci. 32, 538–549.
Zhao, G.C., Sun, M., Wilde, S.A., Li, S.Z., 2003b. Assembly, Accretion and Breakup of the Paleo-Mesoproterozoic Columbia Supercontinent: records in the North China Craton. Gondwana Res. 6, 417–434.
Zhao, G.C., Sun, M., Wilde, S.A., Li, S.Z., 2005. Late Archean to Paleoproterozoic evolution of the North China Craton: key issues revisited. Precambrian Res. 136, 177–202.
Zhao, G.C., Sun, M., Wilde, Li, S.Z., Liu, S.W., Zhang, J., 2006. Composite nature of the North China Granulite-Facies Belt: tectonothermal and geochronological constraints. Gondwana Res. 9, 337–348.
Zhao, G.C., He, Y., Sun, M., 2009. The Xiong'er volcanic belt at the southern margin of the North China Craton: petrographic and geochemical evidence for its outboard position in the Paleo-Mesoproterozoic Columbia Supercontinent. Gondwana Res. 16, 170–181.
Zhao, G.C., Zhai, M.G., 2013. Lithotectonic elements of Precambrian basement in the North China Craton: review and tectonic implications. Gondwana Res. 23, 1207–1240.